UNIVERZITA KARLOVA
FARMACEUTICKÁ FAKULTA V HRADCI KRÁLOVÉ
KATEDRA BIOLOGICKÝCH A LÉKAŘSKÝCH VĚD

RHEINISCHE FRIEDRICH-WILHELMS-UNIVERSITÄT BONN
FACULTY OF MATHEMATICS AND NATURAL SCIENCES
DEPARTMENT OF PHARMACEUTICAL CHEMISTRY

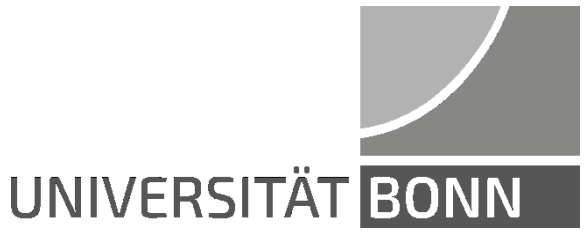

DIPLOMOVÁ PRÁCE
DIPLOMA THESIS

Enzyme kinetic evaluation of several potential inhibitors of certain human cysteine and serine proteases

Hodnocení enzymové kinetiky několika potenciálních inhibitorů lidských proteáz cysteinového a serinového typu

Supervisors:
Prof. Dr. Michael Gütschow
RNDr. Klára Konečná, Ph.D.

2018, Hradec Králové (Czech Republic) **Michaela Hympánová**

DECLARATION

I declare that the enclosed thesis is my original work, and I have not used sources or means without declaration in the text. All thoughts taken directly or indirectly from external sources are properly denoted as such. This work has not been submitted for any other degree or professional qualification.

1 May 2018, Hradec Králové (Czech Republic) ……

ACKNOWLEDGEMENT

I would like to thank prof. Dr. Michael Gütschow for the opportunity to make all my experimental part during my Erasmus internship in his workgroup at the Rheinische Friedrich-Wilhelms-Universität Bonn. He and his colleagues, especially Anna-Christina Schulz-Fincke, Carina Lemke, helped me during experiments. Furthermore, they provided me important guidance during studies and finding methods for my work and consult my whole work. Jim Küppers, Christian Breuer, Seyda Teke and Franziska Kohl provided me their synthesized compounds for experiments. My thanks also belong to my Czech supervisor RNDr. Klára Konečná, Ph.D. for all the help and consultations she provided me.

TABLE OF CONTENTS

1 ABSTRACT IN ENGLISH

Charles University

Faculty of Pharmacy in Hradec Králové

Department of Biological and Medical Sciences

Supervisors: prof. Dr. Michael Gütschow

RNDr. Klára Konečná, Ph.D.

Candidate: Michaela Hympánová

Title of the diploma thesis: Enzyme kinetic evaluation of several potential inhibitors of certain human cysteine and serine proteases

Background

Cysteine and serine proteases are enzymes involved in many physiological processes. The imbalance between them and their endogenous inhibitors is associated with various diseases such as cancer and osteoporosis. Synthetic inactivators could be useful in the treatment of these enzyme-mediated pathological conditions. Therefore, there are ongoing attempts to develop low-molecular weight inactivators for therapeutically relevant cysteine and serine proteases. In the course of this thesis, compounds synthesized in prof. Gütschow's group were investigated as potential inhibitors of selected human proteases. They belong to imidazole compounds derived from *N*-protected cyclohexylalanine, 2-phenyl-7,8-dihydroimidazo[1,2-*a*]pyrazin-6(5*H*)-one derivatives, α,β-unsaturated peptidomimetic compounds, carbamates, an *N,N*-dibenzylcrotonamide derivatives and peptoides.

Aims

This diploma thesis has been focused on the evaluation of new potential inhibitors against human cathepsins B, L, S and K, which belong to cysteine proteases, as well as representatives of serine proteases, human leukocyte elastase and human thrombin. Furthermore, the structure-activity relationships of a small series of low molecular weight compounds were investigated.

Methods

In the experimental part, enzyme inhibition assays and their corresponding kinetic evaluation was introduced. In the course of this project, a human leukocyte elastase inhibition assay was modified and the determination of the Michaelis-Menten constant (K_M) was performed. Based on the obtained data, the inhibitory potency of the tested inhibitors was characterized by methods of linear and non-linear regression analysis to calculate different inhibition parameters.

Results

Most of the imidazole derivatives have shown significant inhibition against human leukocyte elastase. The best inhibitor from this group has been compound **3161** ($IC_{50}/(1 + [S]/K_M)$ = 0.60 ± 0.03 μM) containing a methyl- and phenyl-substituted imidazole moiety. Carbamate **3167** (k_{inac}/K_i = 12.44 $\mu M^{-1}s^{-1}$) was considered as an irreversible cathepsin B inhibitor. The *N,N*-dibenzylcrotonamide derivative, compound **3110** (k_{inac}/K_i = 2292.8 ± 240.74 $\mu M^{-1}s^{-1}$) containing an α,β-unsaturated Michael acceptor substructure, was considered as an irreversible inhibitor of cathepsin K. All other investigated compounds did not show any inhibitory potency.

Conclusion

In summary, some potent inhibitors of some tested enzymes have been found. The imidazole derivatives proved reversible inhibitory potential against human leukocyte elastase. Results with compound **3167** confirmed that the introduction of a carbamate structure is a possible way for the development of new cathepsin B inhibitors. The *N,N*-dibenzylcrotonamide derivative (compound **3110**) demonstrated the potential of Michael acceptors as irreversible cathepsin K inhibitors. Further analogous compounds need to be investigated in the future.

Key words: cathepsins, cysteine proteases, serine proteases, enzyme kinetics, enzyme inhibition

2 ABSTRACT IN CZECH

Univerzita Karlova

Farmaceutická fakulta v Hradci Králové

Katedra biologických a lékařských věd

Školitelé: prof. Dr. Michael Gütschow

RNDr. Klára Konečná, Ph.D.

Kandidát: Michaela Hympánová

Název diplomové práce: Hodnocení enzymové kinetiky několika potenciálních inhibitorů lidských proteáz cysteinového a serinového typu

Úvod

Enzymy řadící se mezi cysteinové a serinové proteázy jsou součástí mnoha fyziologických procesů. Nerovnováha mezi enzymy a jejich endogenními inhibitory patří mezi faktory účastnící se rozvoje řady chorob, například nádorových onemocnění nebo osteoporózy. Syntetické inaktivátory by proto mohly být užitečné v léčbě těchto patologických stavů. Některé látky jsou již ve vývoji a dohledatelné v literatuře. Náplní této diplomové práce je hodnocení inhibičního potenciálu látek syntetizovaných skupinou prof. Gütschowa proti vybraným lidským proteázám. Testované látky patří mezi imidazolové sloučeniny pocházející z *N*-chráněného cyclohexylalaninu, sloučeniny získané substitucí 2-phenyl-7,8-dihydroimidazo[1,2-*a*]pyrazin-6(5*H*)-onu, α,β-nenasycené peptidomimetické sloučeniny, karbamáty, deriváty *N,N*-dibenzyl-krotonamidu a peptoidy.

Cíle

Cílem této diplomové práce bylo zhodnotit nové potenciální inhibitory pomocí testování na katepsinech B, L, S a K, které jsou zástupci cysteinových proteáz a na lidské leukocytární elastáze a trombinu, jakožto zástupcích serinových proteáz. Dalším cílem bylo najít vztahy mezi strukturou látek a potenciálním účinkem.

Metodika

Součástí experimentální části byly metody vedoucí k měření a hodnocení enzymové inhibice. V průběhu experimentu bylo třeba modifikovat metodu měření enzymové aktivity lidské leukocytární elastázy a zároveň stanovit novou Michaelisovu konstantu (K_M) při změněných podmínkách. Na základě získaných dat byly testované látky hodnoceny pomocí lineární a nelineární analýzy a byly vypočteny parametry inhibice.

Výsledky

Většina imidazolových derivátů se prokázala jako reverzibilní inhibitory lidské leukocytární elastázy. Nejsilnější inhibiční účinek z této skupiny měla sloučenina **3161** ($IC_{50}/(1 + [S]/K_M)$ = 0.60 ± 0.03 μM) obsahující imidazol substituovaný fenylem a methylem. Karbamát **3167** (k_{inac}/K_i = 12.44 $\mu M^{-1}s^{-1}$) lze po provedené analýze považovat za ireversibilní inhibitor katepsinu B. Derivát *N,N*-dibenzylkrotonamidu, látka **3110** (k_{inac}/K_i = 2292.8 ± 240.74 $\mu M^{-1}s^{-1}$) obsahující ve své struktuře α,β-nenasycený Michaelův akceptor, může být považována za ireverzibilní inhibitor katepsinu K. Všechny ostatní testované látky neprokázaly inhibiční potenciál.

Závěr

Závěrem můžeme říct, že mezi testovanými látkami byly nalezeny inhibitory některých cílových enzymů. Látky ze skupiny imidazolových derivátů prokázaly reverzibilní inhibiční potenciál proti lidské leukocytární elastáze. Karbamát **3167** poukázal, že sloučeniny tohoto typu by mohly být cestou ve vývoji inhibitorů katepsinu B. Derivát *N,N*-dibenzylkrotonamidu **3110** potvrdil potenciál Michaelova akceptoru jako struktury vhodné u ireverzibilních inhibitorů katepsinu K. Další látky analogické k výše testovaným by měly být syntetizovány a podrobeny enzymatickým testům.

Klíčová slova: katepsiny, cysteinové proteázy, serinové proteázy, enzymová kinetika, enzymová inhibice

3 LIST OF ABBREVIATIONS

αK_i	dissociation constant for enzyme-inhibitor-substrate complex and free inhibitor and enzyme-substrate complex
αK_S	dissociation constant for enzyme-inhibitor-substrate complex and enzyme-inhibitor complex
Ala	alanine
Arg	arginine
AMC	7-amino-4-methylcoumarine
Asn	asparagine
Asp	aspartate
BMD	bone mineral density
Brij. 35	polyethylene glycol dodecyl ether
cat B	cathepsin B
cat K	cathepsin K
cat L	cathepsin L
cat S	cathepsin S
Cys	cysteine
d	offset
DMSO	dimethyl sulfoxide
DTT	dithiothreitol
E	enzyme
EDTA	ethylenediaminetetraacetic acid
EI	enzyme-inhibitor
EIS	enzyme-inhibitor-substrate
ES	enzyme-substrate
Gly	glycine
His	histidine
HLE	human leukocyte elastase
HT	human thrombin
CHAPS	3-[(3-Cholamidopropyl)dimethylammonio]-1-propanesulfonate hydrate

[I]	concentration of inhibitor
IC_{50}	half-maximal inhibitory concentration
K_i	inhibition constant
k_{inac}	first-order rate constant of inactivation
k_{obs}	observed first-order rate constant
K_M	Michaelis-Menten constant
K_S	dissociation constant for enzyme-substrate complex and free enzyme and substrate
Leu	leucine
min	minutes
MES	2-(N-morpholino)ethanesulfonic acid
ODN	odanacatib
[P]	concentration of the product
Phe	phenylalanine
pNA	*para*-nitroaniline
Pro	proline
[S]	concentration of the substrate
S	substrate
S.E.	standard error
suc	succinyl
t	time
Val	valine
v	reaction rate – relative activity of enzyme
v_0	reaction rate in absence of inhibitor
v_i	initial rate
v_{max}	maximum velocity at infinite substrate concentration
v_s	plotting reaction rate – steady-state velocity
x	stoichiometric parameter
Z	carboxybenzyl

4 THE ASSIGNMENT OF DIPLOMA THESIS – OBJECTIVE

The aim of this work was to evaluate the inhibitory potency of several compounds against human cathepsins B, L, S, K, which belong to cysteine proteases, as well as representatives of serine proteases, human leukocyte elastase and human thrombin. It was intended to determinate the structure-activity relationships for small series of low molecular weight compounds. Selective inhibitors could be useful in the treatment of these enzyme-mediated pathological conditions. Moreover, this study was aimed at employing several methods of enzyme kinetic analyses to obtain appropriate kinetic parameters for the observed inhibitory events.

The theoretical part will focus on certain cysteine and serine proteases in general and their therapeutic importance and reasons for development of inhibitors.

The experimental work will include six enzymatic assays for cathepsins B, L, K, S, as well as human leukocyte elastase and human thrombin. Based on the obtained data, the evaluation of the inhibitory activity of the several potential inhibitors will be performed by the analysis of the progress curves. Biochemical parameters of enzyme inhibition will be obtained by methods of linear and non-linear regression analysis. Finally, it is intended to draw structure-activity-relationships for small series of tested low-molecular weight compounds.

5 INTRODUCTION

This thesis is focused on representatives of cysteine and serine proteases, exactly on cathepsins B, L, K, S, human leukocyte elastase and human thrombin. These enzymes are involved in many physiological processes. The imbalance between them and their endogenous inhibitors is associated with various diseases.[1,2] Synthetic inhibitors could be useful in treatment of these pathological conditions. Even according to literature, some inhibitors had already reached clinical trials.[3,4]

In the course of this project potential inhibitors were analyzed by enzyme inhibition assays and their corresponding kinetic evaluation.

6 THEORETICAL PART

6.1 Proteases

Proteases constitute a large group of enzymes capable of catalyzing the hydrolysis of peptide bonds in proteins. They can be classified according to the active site residue of the catalytic triad, *i.e.* serine, cysteine, threonine, aspartyl, glutamic, and metallopeptidases. The proteases can be also divided into exopeptidases and endopeptidases depending on the location of the cleavage within a peptide sequence. Classification according to the role in the organism divides proteases as either degradative, which means that the hydrolysis of peptide bonds leads to complete breakdown of the targeted protein, or regulatory, which means that cleavage of one or more specific bonds alters the biological activity of the targeted protein.[5,6]

Proteases have indispensable roles in various biological processes. In mammalian cells, they are involved in angiogenesis, apoptosis, cell differentiation, immune response, matrix remodeling and protein activation. Imbalance of the enzymes and their endogenous inhibition mechanisms is associated with a number of diseases, including cardiovascular and Alzheimer's disease, cancer, autoimmune diseases, inflammation, and hypertension.[7] This provides the impetus behind the development of new enzyme inhibitors.

Proteolytic enzymes interact with their specific substrates through the specific binding of an amino acid residue with the enzyme's subsites. According to Schechter and Berger nomenclature P1-P1' denotes peptide residues on the acyl and leaving group side of the scissile bond. S1-S1' designate the corresponding subsites of the protease.[8]

Serine and cysteine proteases act directly as nucleophiles by using their catalytic triad to attack an amide carbonyl carbon.[5,6] The cleavage mechanism, a general two-step acyl transfer, is described for the cysteine proteases as follows (Figure 1). The acylation part is initiated by the nucleophilic attack of the thiolate cysteine (A) at the carbonyl carbon of the scissile bond (B) and forms the first tetrahedral intermediate (C) stabilized by the oxyanion hole. The tetrahedral intermediate transforms into an acyl-enzyme (E) with the simultaneous release of the C-terminal portion of the substrate (D). In the subsequent deacylation part, the thiol ester bond of the acyl enzyme is hydrolyzed through the second tetrahedral intermediate (F) which splits into the free enzyme (A) and the N-terminal portion of the substrate (G).[9,10]

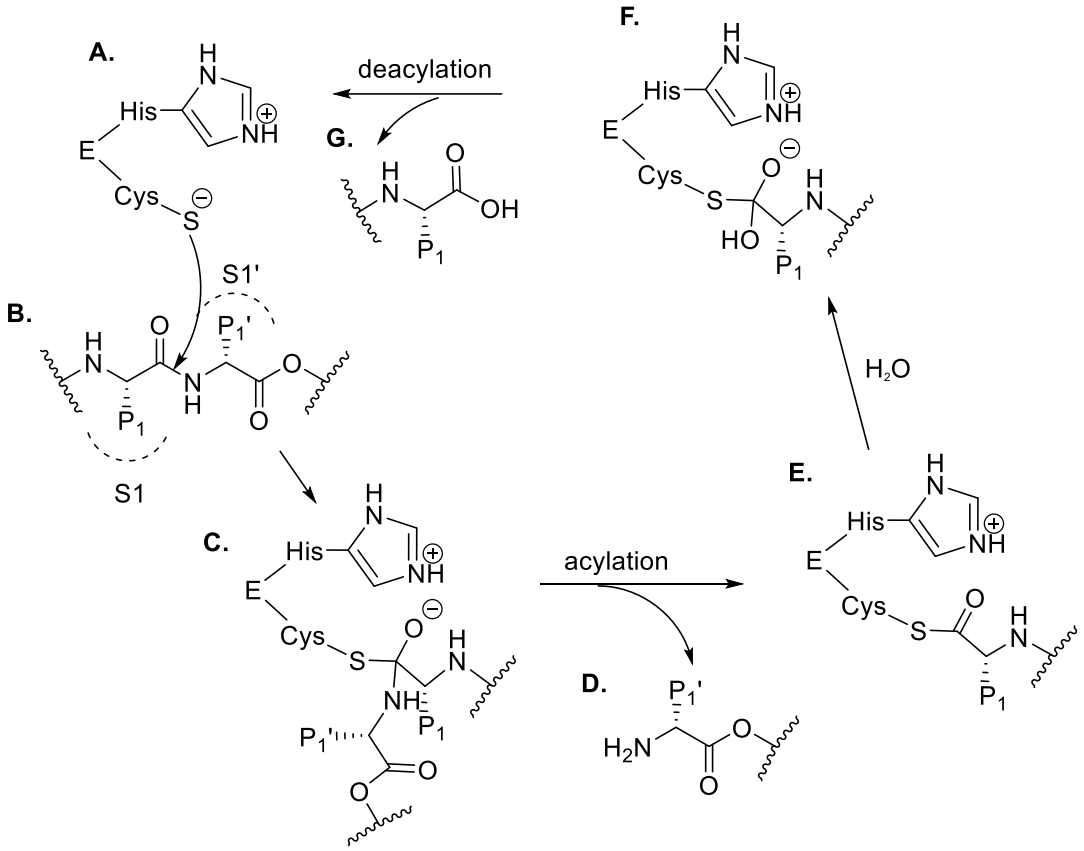

Figure 1: Cysteine protease catalytic mechanism.
The scheme was created by the author of the thesis according to the literature sources.[9,10] Detailed description of the scheme is situated in the previous paragraph.

6.1.1 Cysteine proteases

It has been described 11 human cathepsins B, C, F, H, K, L, O, S, V, W, and X belonging to cysteine proteases.[5,11] The catalytic machinery relies on cysteine-25, histidine-159, and asparagine-175 (papain numbering system).[5,8] Cysteine and histidine forms an ion pair essential for the proteolytic activity of the enzyme and this is stabilized by arginine via a hydrogen bond (Figure 2).[1,9] Human cathepsins are pH-labile cysteine proteases found primarily in lysosomes. The optimum pH for them is slightly acidic, which allows full activity within the lysosomal compartment.[1,9,12] Lysosomal cathepsins are regulated by zymogen activation and by endogenous protein inhibitors.[1] An increase in the level of cathepsin expression and activity is implicated in the development of neurological disorders, cardiovascular diseases, inflammatory diseases such as rheumatoid arthritis, cancer and others.[1,9]

Cathepsin B (cat B) has an occluding loop with two histidine residues which anchors the C-terminal carboxyl group of a substrate. This structure moiety is unique among cathepsins and is related to the endo and exopeptidase activity of cat B.[5] The endopeptidase activity of cat B depends on the flexibility of the occluding loop. Removal of the occluding loop leads to the significant increase in the endopeptidase activity of cat B.[9]

Cathepsin L (cat L) is required in development of hair follicles and skin epidermis, for cardiac morphology and function or for the positive T-cell selection in the thymus.[1] On the other hand, cat L is involved in tumor invasion by degradation of the extracellular matrix and the basal membrane.[6]

Cathepsin S (cat S) and cathepsin K (cat K) show a restricted cell or tissue-specific distribution, which is related to more specific roles in organism.[1] Cat S is selectively expressed in lymphatic tissues and involved in antigen presentation.[1,9]

Cat K is expressed in osteoclasts, in most epithelial cells and in the synovial fibroblasts in rheumatoid arthritis joints.[1,9] The critical role of cat K in bone remodeling is collaborated by the autosomal recessive bone sclerosing disorder, pycnodysostosis (the human form of cat K deficiency) or osteoporosis.[9]

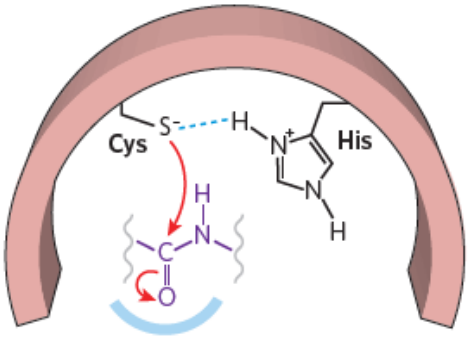

Figure 2: Cysteine protease mechanism.

Catalytic triad is formed by cysteine (Cys), histidine (His) and asparagine (Asn). The nucleophilic attack by the active site cysteine residue in the carbonyl carbon of the scissile bond. The scheme was taken from Erez e t. al., 2009.[13]

6.1.2 Serine proteases

The class of serine proteases is generally well known in the proteases family. Their catalytic triad consists of serine-195, histidine-57, aspartate-102 (papain

numbering system) and its mechanism is comparable to the above mentioned class of cysteine proteases. The nucleophilic attack is executed by the active site serine residue in the carbonyl carbon of the scissile bond (Figure 3). Well-studied members are chymotrypsin, trypsin, elastase, and subtilisin, of which the chymotrypsin-like proteases human leukocyte elastase (HLE) and human thrombin (HT) have been investigated in this thesis.[2,7] These enzymes are part of many critical physiological processes such as digestion, hemostasis, and apoptosis.[2]

HLE is stored in azurophilic granules of neutrophils and capable of breaking down components of the extracellular matrix and foreign proteins. It plays an important role in the innate immune response, in tissue remodeling processes, and in the onset and resolution of inflammation. Out-of-balance HLE activity is associated with many inflammatory diseases, such as chronic obstructive pulmonary disease, adult respiratory distress syndrome or cystic fibrosis.[14,15]

HT plays an important role in coagulation, anticoagulation and fibrinolysis.[16] The anticoagulation therapy is a main part of modern medical therapy for cardiovascular and thrombotic diseases. Direct HT inhibitors are a class of anticoagulants that binds directly to HT and inhibits its interaction with substrates.[17] Recombinant hirudins belong to parenteral direct HT inhibitors. Dabigatran represents an oral specific and reversible inhibitor.[18]

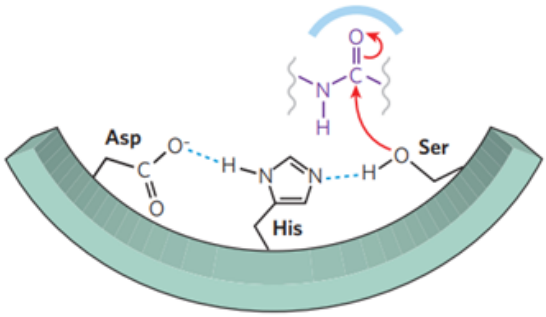

Figure 3: Serine protease mechanism.

Catalytic triad is formed by serine (Ser), histidine (His) and aspartate (Asp). The nucleophilic attack by the active site serine residue in the carbonyl carbon of the scissile bond. The scheme was taken from Erez et. al., 2009.[13]

6.2 Enzyme inhibitors in drug development

Enzymes are commonly the target of new drug discovery, thanks to their essential roles in many diseases. The active site of the enzymes, responsible for the catalytic activity, can often be inhibited by small molecules. Enzyme inhibitors represent almost half of the drugs in the clinical use today. A few examples are given in Table 1.[19]

Table 1: Selected enzyme inhibitors in clinical use.[19]

Compound	Target enzyme	Clinical use
Allopurinol	Xanthine oxidase	Gout
Aspirin	Cyclooxygenases	Inflammation, pain, fever, anticoagulation
Clavulanate	β-Lactamase	Co-drug for ATB
Methotrexate	Dihydrofolate reductase	Cancer, immunosuppression
Omeprazole	H^+, K^+ ATPase	Peptic ulcers

The examples of direct HT inhibitors, as participating enzyme in this thesis, are previously mentioned to be recombinant hirudins and dabigatran as anticoagulants.[18] Sivelestat, as HLE inhibitor, reached a phase IV study in treatment of acute lung injury associated with systemic inflammatory response syndrome.[4] Some other research groups have published articles about their work with potentials HLE inhibitors.[20,21] Based on known literature, no inhibitors of cathepsins B, L, S and K are in clinical use. Most progress was found in the field of drug development of cat K inhibitors. The importance of cat K in bone resorption led to the assumption that specific cat K inhibitors will be beneficial in the treatment of osteoporosis.[9] For example, balicatib (Figure 4) has been subjected to phase II clinical trials. Favorable effects on the reduction of relevant biochemical markers of bone resorption and an increase in bone mineral density was observed. Besides this, also skin adverse events as pruritus, rashes and rare morphea-like skin changes were manifested. Another promising compound, odanacatib (ODN) (Figure 4), underwent clinical trials within the last years which will be shortly introduced in the next chapter.[22]

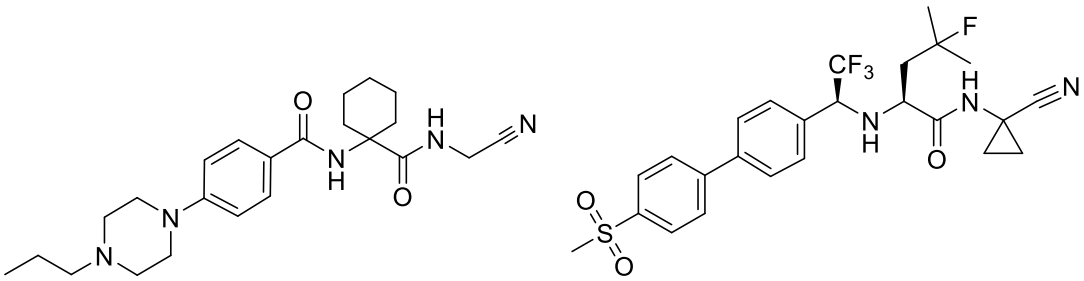

Figure 4: Left: chemical structure of balicatib.[23] Right: chemical structure of odanacatib.[3]

6.3 Cathepsin K inhibitors and osteoporosis

In the human skeleton, there is normally a balance between bone resorption and formation.[24] Osteoporotic bones are characterized by increased bone resorption and diminished bone formation, which leads to a reduction in bone mineral density (BMD) and increases the risk of developing fractures.[25] During the bone resorption, osteoclasts secrete protons onto the bone surface, which causes demineralization of the membrane. Further, cat K disrupts an exposed organic matrix primarily containing collagen type 1.[26] A simplified scheme of bone resorption is given in Figure 5.

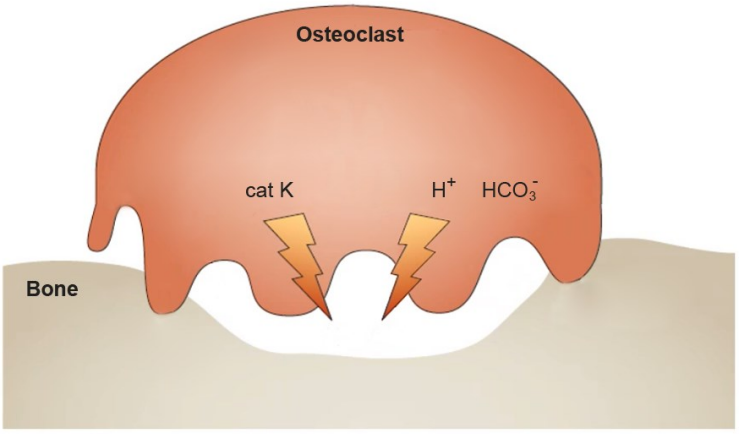

Figure 5: Bone resorption.
Protons secreted by osteoclasts causes demineralization of the bone surface membrane. Cathepsin K (cat K) disrupts an exposed organic matrix. The Figure was created by the author of the thesis according to the literature sources.[24,26]

The selective inhibitor of cat K, odanacatib, was developed for osteoporosis treatment on postmenopausal women with low BMD.[27–33] In the following paragraphs, the results of clinical trials in phases II and III are described.

In the phase II clinical trial, the drug is first administered to a small number of patients and the main emphasis is given on safety and efficiency. The therapeutic effects are demonstrated, a suitable dose is sought, and additional drug data are collected.[34]

For this purpose, four follow-up studies were conducted of weekly oral ODN (up 50 mg) for up to 8 years. BMD and biomarkers of skeletal remodeling were observed. Two last study extensions up to 5 and 8 years had limitations because of the small number of patients remaining in each treatment group, which prevented formal statistical analysis, as originally described in the study design. The lack of randomization (patients were carried over from their originally assigned treatment) and the open-label nature of this extension may have caused additional bias. These clinical trials had shown a dose-dependent increase in BDM at multiple sites. Improvements in BMD were generally greatest in those patients who had received continuous ODN 50 mg for the longest period of time. Whereas bone resorption markers remained reduced, no significant change was observed in bone formation markers. During the first 6 months, ODN transiently suppresses bone-formation markers. They returned to baseline levels by the end of second year despite continued treatment and both remained at or near baseline during the third year of treatment. Other osteoclast activities did not appear to be greatly affected. Inhibition of cat K enzyme activity by ODN is a reversible process and BMD returns to baseline levels or slightly below after discontinuation of treatment.[27–30] Results of treatment with the 3 mg dose of ODN were contrary to expectations and contrary to what was observed at higher doses. An accelerated bone turnover was observed and the BMD results were similar to placebo. The lack of benefit from the 3 mg weekly dose may have resulted from insufficiently sustained suppression of cat K throughout the duration of the weekly dosing interval. As such, this had been a theoretical concern in patients, who had been noncompliant with the standard dose or who had had faster drug metabolism.[28]

Phase III trial typically involves hundreds to thousands of patients in order to verify the efficiency and to get more information about the safety.[34]

For this purpose, the next 2-years trial with 214 postmenopausal women with low BMD had been performed. In women treated weekly by 50 mg for 2 years, ODN demonstrated a consistent effect relative to placebo.[31] Another long-term ODN phase III

trial was performed on more than 16,000 postmenopausal women with low BMD. Patients had received ODN 50 mg for 3 years. The study showed a robust reduction in fracture incidence. The trial was stopped early after a planned analysis had shown robust efficacy and a favorable benefit/risk profile.[32]

Unfortunately, analysis of clinical data showed that while ODN had been indeed effective, it also increased the risk of a stroke. In September 2016, Merck announced that they discontinued the development of the compound.[33]

Despite the above-mentioned compounds eventually failed in their trials, the path of possible success did not end here. Research groups such as the one of prof. Michael Gütschow continue in the development of new promising substances in this area.

7 EXPERIMENTAL PART

7.1 Material

Substrates Z-Arg-Arg-pNA, Z-Phe-Arg-pNA, Z-Leu-Arg-AMC, Z-Phe-Arg-AMC and Z-Gly-Gly-Arg-AMC were purchased from Bachem (Switzerland). Substrate MeO-Suc-Ala-Ala-Pro-Val-pNA was obtained from abcr GmbH (Germany). Used abbreviations can be found in the list of abbreviations at the page 10.

Human cat B was purchased from Calbiochem (Germany). Human cat L and cat K and human recombinant cat S were obtained from Enzo Life Science (Germany).

NaH_2PO_4 and Na_2HPO_4 for sodium phosphate buffer, citric acid and trisodium citrate for sodium citrate buffer, NaCl and dimethyl sulfoxide (DMSO) were obtained from Fisher Scientific. Polyethylene glycol dodecyl ether (Brij. 35), 3-[(3-Cholamidopropyl)dimethylammonio]-1-propanesulfonate hydrate (CHAPS), Triton-X, ethylenediaminetetraacetic acid (EDTA) from Applichem GmbH (Germany). 2-(*N*-morpholino)ethanesulfonic acid (MES), dithiotreitol (DTT) from Carl Roth GmbH (Germany).

96-well plate with flat bottom, pipette tips 0.2-20 µL, 20-200 µL, 100-100 µL were purchased from Sarstedt (USA). Plastic Eppendorf tubes, spatulas for mixing and disposable cuvettes Carl Roth were obtained from GmbH (Germany).

7.2 Instruments

Fluorometric assays were performed in a using a FLUOstar Optima (BMG LABTECH, Germany). A Cary® 50 UV-Vis (Varian, INC., Agilent Technologies, Nederland) spectrophotometer was used for spectrophotometric measurements.

7.3 Methods

Compounds were investigated with concentration 5 µM or 1 µM (depending on solubility) in duplicates. In case of obtained inhibition 5 different inhibitor concentrations were investigated in duplicates or with 10 different inhibitor concentrations in a single measurement. Depending on the type of inhibition, the obtained progress curves were analyzed by linear or non-linear regression.

At first frozen enzymes were activated. Liquid cathepsins B, L, K and S were diluted and incubated with activating buffer under the certain condition according to

each assay instruction. In case of HT and HLE, only dilution with assay buffer was performed. Activated enzymes were always kept in a box with ice. An exception was direct dilution of HLE before every measurement, because of the fast activity decrease of this enzyme.

Stock solution of the substrates and inhibitors were always prepared in DMSO. The exception was one more dilution of substrate in HLE assay with DMSO and assay buffer.

In every spectrometric or fluorometric measurement cuvettes or well plates were prepared in the same order (Figure 6). The assay buffer, DMSO, inhibitor and substrate stock solution were added in this order and volume was subsequently mixed. Enzyme was added as the last one and volume was again thoroughly mixed.

Every measurement had two controls containing everything without inhibitor. Duplicate measurements were made in different runs under the same conditions.

For easier orientation in cuvettes or well plates preparation, it was advisable to prepare a table containing volume of individual substances (example in Table 2).

Detailed descriptions of each assay are given in the following paragraphs.

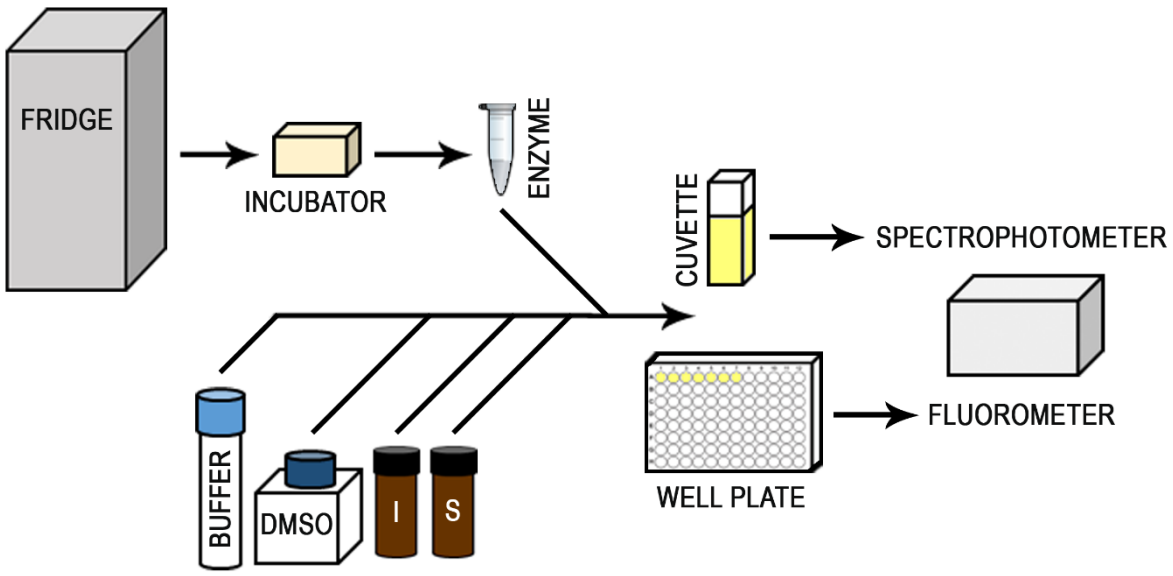

Figure 6: Scheme of assays.

The enzymes belonging to this thesis were stored in the refrigerator. For an enzymatic activation they were incubated under certain conditions in the incubator. The cuvettes were subsequently filled up by assay buffer, dimethyl sulfoxide (DMSO), inhibitor (I) and substrate stock solution (S) in this order. The volume was subsequently mixed and

the enzyme was added as the last one. The volume was thoroughly mixed again and cuvettes were given into the spectrophotometer and well plate into the fluorometer. Measurements were performed under certain conditions according to each enzymatic assay (described in the following paragraphs). The scheme was created by the author of the thesis.

Table 2: Cathepsin B assay

	Assay buffer [µL]	**DMSO [µL]**	**Inhibitor 10 mM [µL]**	**Substrate [µL]**	**Activated and diluted enzyme [µL]**
Control	960	15	0	5	20
Inhibitor 5 µM	940	14.5	0.5	5	20

The example of table containing the correct volume of the each substance according to cathepsin B assay for measurement of control inhibitor at concentration of 5 µM. Table was made by the author of the thesis.

7.3.1 Mechanism of detection

The activity of the enzyme is based on the absorbance or fluorescence of the formed product. During the spectrophotometric measurement, *para*-nitroaniline (pNA) is cleaved from the chromogenic substrate by the enzyme. Absorbance of yellow pNA is observed, and according to Lambert-Beer law, is directly equal to the product concentration. In the fluorescence method, the fluorophore 7-amino-4-methylcoumarine (AMC) is the part cleaved by enzyme from the fluorogenic substrate. Amino acids in the individual substrates are selected according to the preferences of the individual enzyme. The schematic equations of the reactions are shown in Figure 7.

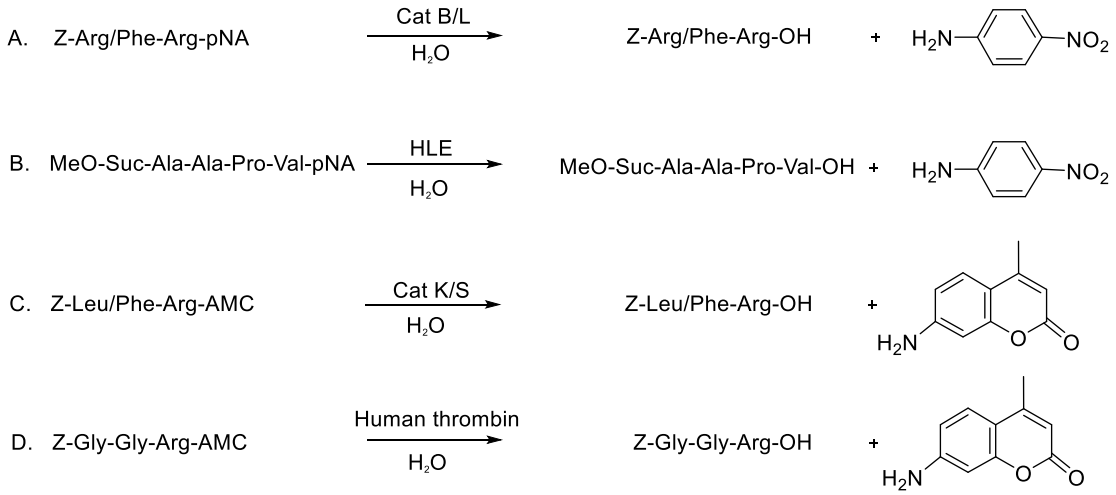

Figure 7: Scheme of enzyme reactions.

A, B: Spectrophotometric reaction mechanism performed with human leukocyte elastase (HLE), cathepsin B (cat B) and cathepsin L (cat L). Yellow *para*-nitroaniline (pNA) is released from the substrate after enzymatic cleavage. C, D: Fluorescent reaction mechanism performed with cathepsin K (cat K) and cathepsin S (cat S), as well as HT. Fluorescent 7-amino-4-methylcoumarineis (AMC) is released from the substrate after enzyme cleavage. Z is representing the carboxybenzyl as an amine protecting group. Abbreviations of amino acids are described in the list of abbreviations (page 10). The Figure was created by the author of the thesis.

7.3.2 Human cathepsin B inhibition assay

The cathepsin B assay[35] was based on spectrophotometric measurements of the released pNA at wavelength 405 nm and 37 ºC (the reaction scheme in Figure 7, page 25).

The assay buffer was composed of 100 mM sodium phosphate buffer (pH 6.0), 100 mM NaCl, 5 mM EDTA and 0.01% Brij. 35.

The enzyme stock solution of the human cathepsin B with the concentration of 0.47 mg/mL was prepared in 20 mM sodium acetate buffer (pH 5.0) and 1 mM EDTA and kept at 0°C.

The substrate Z-Arg-Arg-pNA stock solution with the concentration of 100 mM was made in DMSO.

The inhibitor stock solution was prepared in DMSO.

At first the enzyme was activated according to subsequent process. The enzyme stock solution was diluted in proportion 1:500 in assay buffer additionally containing 5 mM DTT and was incubated for 30 min at 37 ºC.

Subsequently cuvettes were prepared. Each cuvette contained 960 µL of the assay buffer, 15 µL of the inhibitor solution and DMSO in total and 5 µL of the substrate solution. Then the cuvette volume was mixed and the catalytic transformation of the substrate started after adding 20 µL of the activated enzyme solution. The conclusive concentration of the substrate was 500 µM (= 0.45 K_M), while the conclusive concentration of cathepsin B was 18.8 ng/mL and 2 % of the DMSO in the cuvette. The value of K_M was taken from the original assay.[35] The reactions were followed over 60 min. All experiments were performed in duplicates.

7.3.3 Human cathepsin L inhibition assay

The cathepsin L assay[35] was based on spectrophotometric measurements of the released pNA at wavelength 405 nm and 37 ºC (the reaction scheme in Figure 7, page 25).

The assay buffer was composed of 100 mM sodium phosphate buffer pH 6.0, 100 mM NaCl, 5 mM EDTA and 0.01% Brij 35.

The enzyme stock solution of human cathepsin L with the concentration of 135 µg/mL was prepared in 20 mM malonate buffer pH 5.5, 400 mM NaCl, and 1 mM EDTA and kept at 0°C.

The substrate Z-Phe-Arg-pNA stock solution with the concentration of 10 mM was made in DMSO.

The inhibitor stock solution was prepared with DMSO.

At first the enzyme was activated according to subsequent process. The enzyme stock solution was diluted in proportion 1:100 in assay buffer additionally containing 5 mM DTT and was incubated for 30 min at 37 ºC.

Subsequently the cuvettes were prepared. Each cuvette contained 940 µL of the assay buffer, 10 µL of the inhibitor solution and DMSO in total and 10 µL of the substrate solution. Then the cuvette volume was mixed and the catalytic transformation of the substrate started after adding 40 µL of the activated cathepsin L solution. The final concentration of the substrate was 100 µM (= 5.88 K_M), the conclusive concentration of cathepsin L was 54 ng/mL and the final concentration of DMSO was

2 %. The value of K_M was taken from the original assay.[35] The reactions were followed over 60 min. All experiments were performed in duplicates.

7.3.4 Human cathepsin K inhibition assay

The cathepsin K assay[35] was carried out fluorometrically at 25 °C in a 96-well plate with flat bottom with adjusted wavelength of 360 nm for excitation and 440 nm for emission (the reaction scheme in Figure 7, page 25).

The assay buffer consists of 100 mM sodium citrate pH 5.0, 100 mM NaCl, 1 mM EDTA and 0.01% CHAPS.

The enzyme solution of human cathepsin K with the concentration of 23 μg/mL was prepared in 50 mM sodium acetate pH 5.5, 50 mM NaCl, 0.5 mM EDTA and 5 mM DTT and kept at 0°C.

The substrate Z-Leu-Arg-AMC stock solution with the concentration of 10 mM was made in DMSO.

The inhibitor stock solution was prepared with DMSO.

At first the enzyme was activated according to the subsequent process. The enzyme stock solution was diluted in proportion 1:100 in assay buffer additionally containing 5 mM DTT and was incubated for 30 min at 37 ºC.

Subsequently well plate was prepared. Into each well containing 192 μL of the assay buffer, 3.2 μL of the inhibitor solution and DMSO in total and 0.8 μL of the substrate solution were added and thoroughly mixed. The reaction was initiated by adding 4 μL of the activated cathepsin K solution. The final concentration of the substrate was 40 μM (= 13.3 K_M), the conclusive concentration of cathepsin K was 5 ng/mL and the final concentration of DMSO was 2 %. The value of K_M was taken from the original assay.[35] The reactions were followed over 60 min. All experiments were performed in duplicates.

7.3.5 Human cathepsin S inhibition assay

Human recombinant cathepsin S[36] was assayed fluorometrically at 25 °C in a 96-well plate with flat bottom with adjusted wavelength of 360 nm for excitation and 440 nm for emission (the reaction scheme in Figure 7, page 25).

The assay buffer consists of 100 mM sodium phosphate buffer pH 6.0, 100 mM NaCl, 5 mM EDTA, and 0.01% Brij 35.

The enzyme solution of human recombinant cathepsin S with the concentration of 70 μg/mL was prepared in 100 mM MES buffer, pH 6.5, 1 mM EDTA, 50 mM L-cysteine, 10 mM DTT, 0.5% Triton X-100 and 30% glycerol and kept at 0 °C.

The substrate Z-Phe-Arg-AMC stock solution with the concentration of 10 mM was made in DMSO.

The inhibitor stock solution was prepared with DMSO.

At first the enzyme was activated according to subsequent process. The enzyme stock solution was diluted in proportion 1:100 in with another buffer containing 50 mM sodium phosphate buffer pH 6.5, 50 mM NaCl, 2 mM EDTA, 0.01% Triton X-100 and 5 mM DTT and was incubated for 60 min at 37 ºC.

Subsequently well plate was prepared. Into each well containing 184 μL of the assay buffer, 3.2 μL of the inhibitor solution and DMSO in total and 0.8 μL of the substrate solution were added and thoroughly mixed. The reaction was initiated by adding 12 μL of the activated cathepsin S solution. The final concentration of the substrate was 40 μM (= 0.74 K_M), the conclusive concentration of cathepsin S was 42 ng/mL and the final concentration of DMSO was 2 %. The value of K_M was taken from the original assay.[36] The reactions were followed over 60 min. All experiments were performed in duplicates.

7.3.6 Human thrombin inhibition assay

HT was assayed[37] fluorometrically at 25 °C in a 96-well plate with flat bottom with adjusted wavelength of 340 nm for excitation and 460 nm for emission (the reaction scheme in Figure 7, page 25).

Assay buffer was 50 mM Tris-HCl, 150 mM NaCl, pH 8.0.

The enzyme solution of HT with the concentration of 1000 U/mL was prepared in water, kept at 0 °C and at the beginning of measurement was diluted with assay buffer.

A 10 mM stock solution of fluorogenic substrate Z-Gly-Gly-Arg-AMC in DMSO was diluted with assay buffer to concentration of 800 μM.

Into each well containing 173.8 μL assay buffer, 11.2 μL of the inhibitor solution and DMSO in total and 10 μL of substrate solution (800 μM) were added and

thoroughly mixed. The reaction was initiated by adding 5 µL of enzyme solution (100 U/mL). The final concentration of the substrate in well was 40 µM (= 1.00 K_M), of DMSO was 6 % and of HT was 2.5 U/mL. The value of K_M was taken from the original assay.[37] The reactions were followed over 10 min. All experiments were performed in duplicates.

7.3.7 Human leukocyte elastase inhibition assay

The HLE assay[38] was based on spectrosphotometric measurements of the released pNA at wavelength 405 nm and 25 ºC (the reaction scheme in Figure 7, page 25).

Assay buffer was 50 mM sodium phosphate buffer, pH 7.8.

100 µg/mL enzyme stock solution was prepared in 100 mM sodium acetate buffer, pH 5.5.

The substrate MeO-Suc-Ala-Ala-Pro-Val-pNA stock solution with the concentration of 50 mM was made in DMSO and assay buffer. The final concentration of the substrate in this stock solution was 2 mM and 10 % of DMSO.

The inhibitor stock solution was prepared with DMSO.

Into each well containing 890 µL assay buffer, 10 µL of the inhibitor solution and DMSO in total and 50 µL of substrate solution were added and thoroughly mixed. The reaction was initiated by adding 50 µL of enzyme solution. The final concentration of the substrate was 100 µM (= 1.85 K_M) and the final concentration of DMSO was 1.5 %. The conclusive concentration of HLE was 0.08 µM (depend on relative activity of enzyme). Dilution of enzyme solution to required concentration had to be done directly before every measurement in cold assay buffer. The value of K_M was taken from the original assay.[37] The reactions were followed over 10 min. All experiments were performed in duplicates or once at 10 different concentrations of a compound.

Due to the poor solubility of imidazole compounds derived from *N*-protected cyclohexylalanine was this assay optimized and compounds were measured in the presence of 2.5 % of DMSO. In each cuvette, there was 880 µL of assay buffer and 20 µL of the inhibitor solution and DMSO in total and 50 µL of substrate solution. The final concentration of the substrate in the cuvette was still 100 µM (= 0.96 K_M), while the conclusive concentration of DMSO was 2.5 %. The value of K_M was determined. Determination and optimization details are described at page 35.

7.4 Enzyme kinetic evaluation of inhibitory activity

Data evaluations according to the following equations (graphs and results) were performed by the author of the thesis in GraFit - data analysis software for Windows. Chemical structures were made by the author of the thesis in ChemDraw® Professional - chemistry software.

Progress curves obtained in the kinetic experiments reflects the product formation during the measurement.

In each measurement, the product formation of the control (100 %) was used to calculate the product formation in the presence of the inhibitor (%). The half-maximal inhibitory concentration (IC_{50}) values can be calculated from the percentile activity according to the equation 1 (Figure 15, page 38). A value of activity for another concentration of inhibitor can be estimated from the IC_{50} according to the same equation.[39]

Analysis of the progress curves depends on the binding mode of the inhibitor. In the course of this thesis, it was distinguished between reversible and irreversible inhibition, and the corresponding evaluation was performed as described below.[39]

7.4.1 Reversible inhibition

The enzymatic reaction begins with the formation of the enzyme-substrate (ES) complex from the substrate (S) and the free enzyme (E). This reaction is quantified by the dissociation constant K_S. Reversible formation of the enzyme-inhibitor (EI) complex is driven by non-covalent interactions between the enzyme and the inhibitor and can be divided into three modes. The first competitive mode is described by inhibitor binding to enzyme, in direct competition with the substrate. The equilibrium between EI complex and free enzyme and inhibitor molecules is determinated by the dissociation constant K_i. Noncompetitive inhibitors display binding affinity for both the free enzyme and the ES complex. In that case, another dissociation constant αK_i for enzyme-inhibitor-substrate (EIS) complex has to be described. The α constant defines the effect of the inhibitor to enzyme affinity to the substrate. The last uncompetitive inhibitor binds exclusively to the ES complex.[19] The general mechanism is shown in Figure 8.

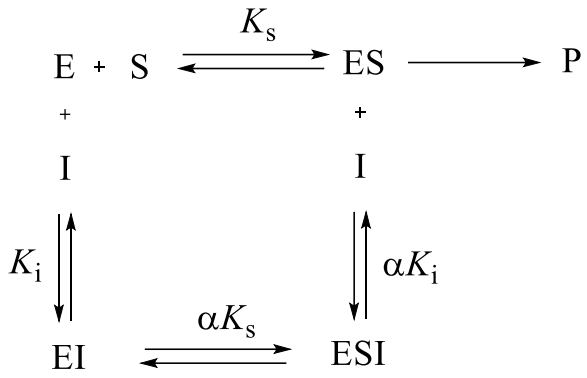

Figure 8: Scheme of reversible inhibition.[19]

E is the enzyme, S is the substrate, I is the inhibitor, P is the product and K_S, K_i, αK_i and αK_S are the dissociation constants. The scheme was made by the author of the thesis according to literature sources.[19]

Reversible inhibition is represented by linear progress curves of the product formation. Linear regression can be used for the evaluation as shown in Figure 9.

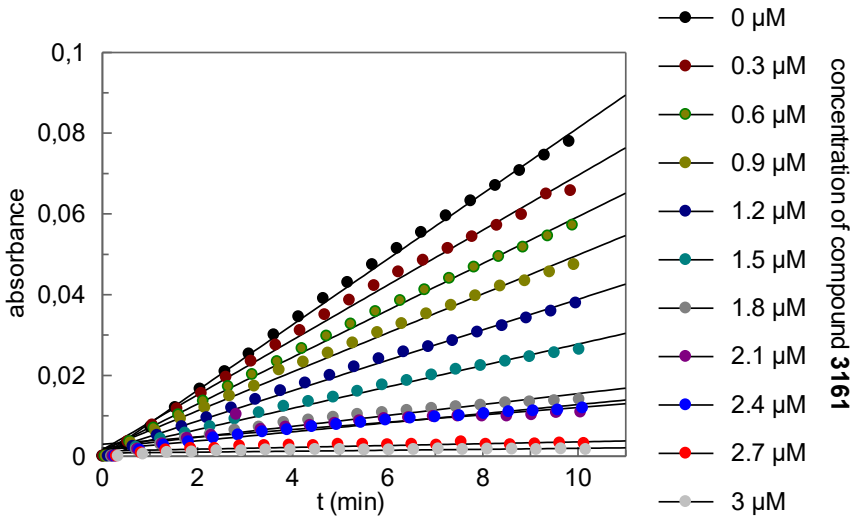

Figure 9: Progress curves at presence of reversible inhibitor.

Inhibition of human leukocyte elastase by an imidazole compound derived from *N*-protected cyclohexylalanine (**3161**). The enzyme activity depends on the concentration of the inhibitor. The progress curves can be analyzed by linear regression.

Relative activity (v) of the enzyme at individual inhibitor concentrations was calculated according to the equation 2 (Figure 15, page 38) and used for determination of IC_{50} values by two different models. IC_{50} values were obtained by non-linear

regression according to same equation, where v is the reaction rate in the presence of the inhibitor, v_o is the rate in the absence of the inhibitor, x indicates an imbalance in the reaction stoichiometry.[39]

The second method to calculate the IC_{50} value was based on the same equation, but required that the reaction stoichiometry is 1:1, thus x = 1. The equation is simplified to a two-parameter equation.[39] The graphical representation of both methods is shown in Figure 10 with compound **3161.**

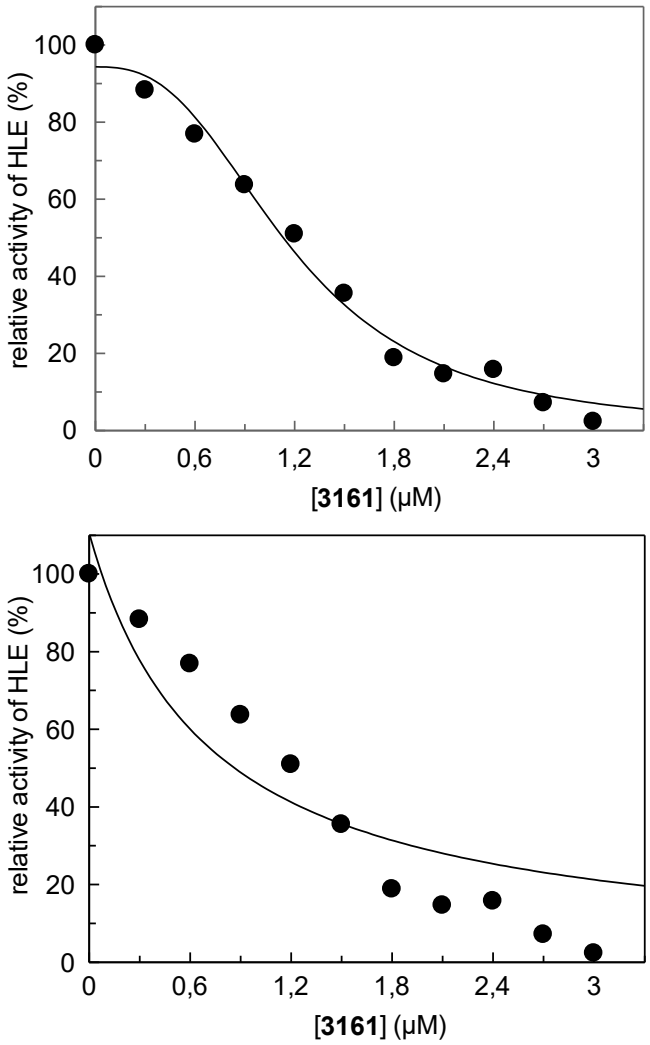

Figure 10: IC_{50} determination by two different methods.
Relative enzyme activities plotted against inhibitor concentrations. Upper: A three-parameter equation was used. Lower: A two-parameter equation was used.

The obtained results are not comparable with different assays because IC_{50} values depend on the substrate concentration. For comparability, IC_{50} values should be corrected by the factor of $(1 + [S]/K_M)$, where [S] is the substrate concentration and K_M is the Michaelis-Menten constant. In general, the K_M value is determined under the

assay conditions and characterizes the affinity of the enzyme for the specific substrate under these conditions. The conversion of IC_{50} values to K_i values is based on the Cheng-Prusoff equation 3 (Figure 15, page 38) which is valid for a competitive enzyme inhibition.[19]

7.4.2 Irreversible inhibition

Irreversible inactivators form a covalent bond after the nucleophilic attack to the target enzyme which results in a time-dependent inhibition. Hyperbolic progress curves are expected and can be analyzed by non-linear regression using the equation 4 (Figure 15, page 38).[19] An example, inhibition of cathepsin B by compound **3110**, is given in Figure 11.

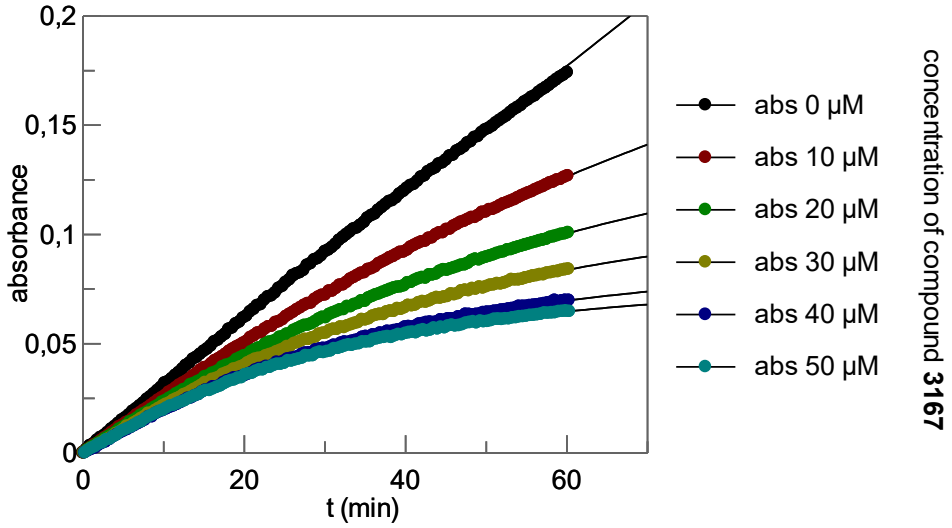

Figure 11: Progress curves in presence of irreversible inhibitor.
A concentration-dependent inhibition of cathepsin B by **3167**. The product formation was monitored in the presence of different inhibitor concentrations. The progress curves were analyzed by non-linear regression.

The rate at which the enzyme is inactivated is determined by the first-order rate constant k_{obs} according to the equation 4 (Figure 15, page 38). First-order rate constant of inactivation (k_{inac}) defines the maximum rate of inactivation that is achieved at infinite concentration of inhibitor. [19]

For evaluation, the obtained k_{obs} values were plotted versus increasing inhibitor concentrations to obtain k_{obs}/[I] values. From k_{obs}/[I], the second order rate parameter k_{inac}/K_i can be calculated. The K_i defines the concentration of inhibitor that yields a rate

of inactivation that is equal to ½ $k_{inac.}$ If the measured inhibitor concentrations are below K_i, the linear dependence of k_{obs}/[I] can be observed and k_{inac}/K_i can be calculated according to the equation 5 (Figure 15, page 38), where the inhibitor concentration is not included in the denominator compared to the equation 6 (Figure 15, page 38). Yet, non-linear regression is performed in case the used inhibitor concentrations are about the K_i to obtain the k_{inac}/K_i according to the equation 6 (Figure 15, page 38). Examples of these different types of evaluations are given in Figure 12.[19]

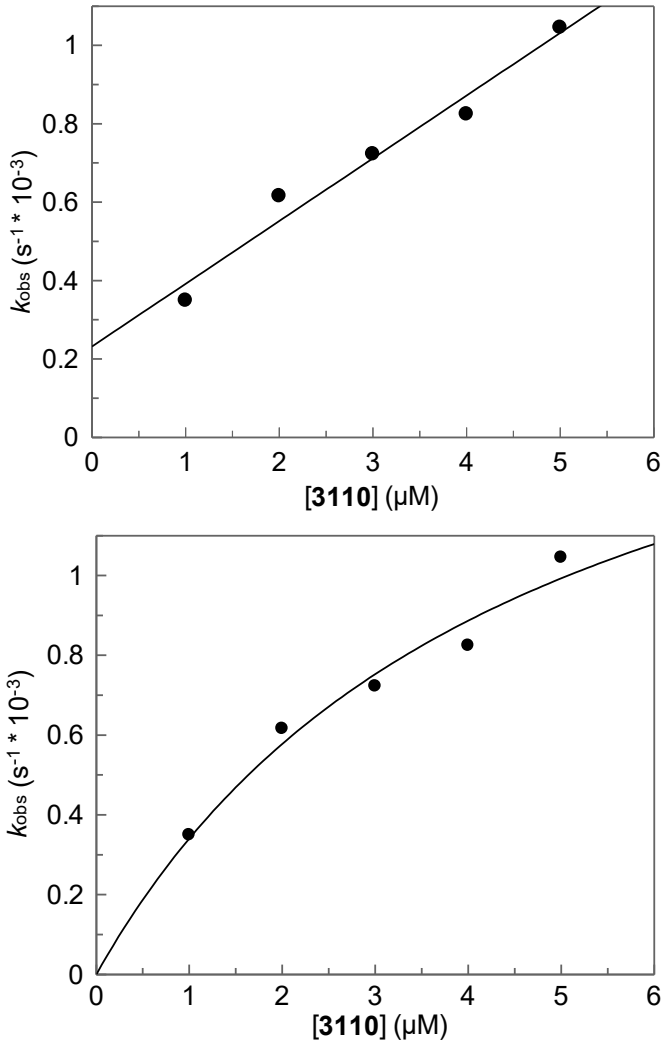

Figure 12: The values k_{obs} plotted against the different concentrations of the inhibitor. Inactivation of cathepsin K by **3110**. Upper: The inhibitor concentrations are below K_i. Lower: The inhibitor concentrations are around the K_i.

7.4.3 Determination of the Michaelis-Menten constant

The Michaelis-Menten constant (K_M) is the substrate concentration at which the reaction rate is at half of the maximum. It characterizes the affinity of the enzyme for the specific substrate under the specific assay conditions.

The tested imidazole compounds derived from *N*-protected cyclohexylalanine showed limited solubility during measurements with HLE. Therefore, assay conditions were optimized by increasing the final concentration of DMSO from 1.5 % to 2.5 %. Thus, a new K_M value had to be determined.

HLE activity was assayed over 10 minutes with 20 different substrate concentrations in triplicate measurements. The chromogenic substrate used in the HLE assay was MeO-Suc-Ala-Ala-Pro-Val-pNA. The assay was carried out at pH 7.8 and 25 °C.

For K_M determination is necessary to obtain the steady-state velocities (v_s) of progress curves at each measured substrate concentration. The K_M was calculated to be 104.11 ± 7.13 µM by plotting reaction rate (steady-state velocity) against substrate concentration and using nonlinear regression according to the Michaelis-Menten equation (equation 7, Figure 15, page 38). Graphs and kinetic evaluation were made by the author of the thesis in GraFit - data analysis software for Windows (Figure 14).

In the course of this thesis second determination of K_M by Hanes-Woolf plot (Figure 13 and 14) was performed. This linear method is less accurate, but easier for visualization. The Hanes-Woolf plot, where $[S]/v_s$ is plotted versus substrate concentration is given in Figure 14. Linear regression gave the K_M value of 99.18 ± 6.71 µM.[40]

This result can be compared with the K_M value of 54.05 µM from in the before used HLE assay. A higher K_M value means, that a higher substrate concentration is needed to reach half of the maximum rate, reflecting a decreased enzyme affinity for the substrate. An increase in DMSO from 1.5 % to 2.5 % increased the K_M value almost twice. The reduced affinity of HLE for the MeO-Suc-Ala-Ala-Pro-Val-pNA substrate could be expected, because DMSO likely has a negative impact on the enzyme-substrate interaction.

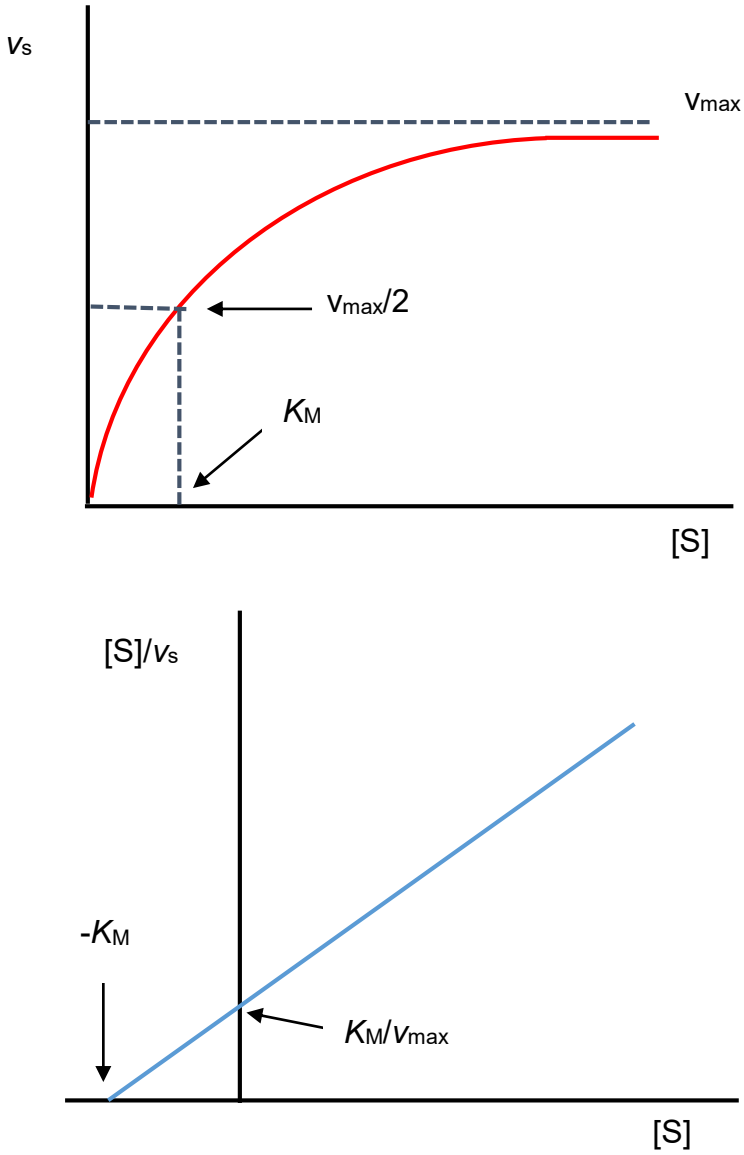

Figure 13: Determination of the Michaelis-Menten constant

Upper: Plotting reaction rate (steady-state velocity - v_s) against substrate concentration [S] by using nonlinear regression according to the Michaelis-Menten equation (equation 7, Figure 15, page 38) v_{max} is maximum velocity obtained at infinite substrate concentration, K_M is the Michaelis-Menten constant. Lower: Linear evaluation by Hanes-Woolf plot, where [S]/v_s is plotted versus substrate concentration. Figures were made by the author of the thesis according to literature sources.[19,40]

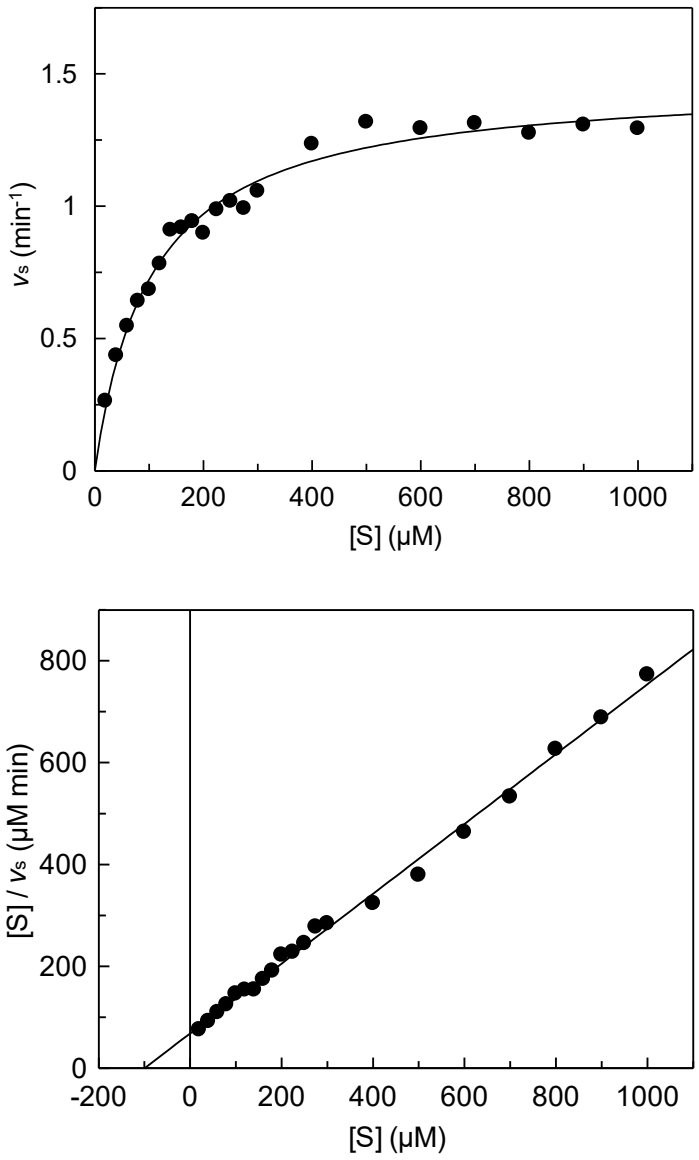

Figure 14: Result of Michaelis-Menten constant determination.

For the HLE-catalyzed cleavage of the MeO-Suc-Ala-Ala-Pro-Val-pNA. HLE was assayed spectrophotometrically in cuvettes at 405 nm and at 25 °C. Assay buffer was 50 mM sodium phosphate buffer, pH 7.8. Final DMSO concentration was 2.5 %. 20 various substrate concentrations were measured in triplicates for 10 minutes. Upper: Plot of steady-state reaction rates (v_s) as a function of substrate concentration [S]. Michaelis-Menten constant (K_M) value of 104.1 ± 7.1 μM was obtained. Lower: Hanes-Woolf plot, where [S]/v_s is plotted versus substrate concentration. K_M value of 99.18 ± 6.71 μM was obtained. Graphs and kinetic evaluation were made by the author of the thesis in GraFit - data analysis software for Windows.

7.4.4 General equations

1. $\mathrm{IC_{50}} = [\mathrm{I}]/\left(\frac{v_0}{v} - 1\right)$
2. $v = v_0/\left(1 + \left(\frac{[\mathrm{I}]}{\mathrm{IC_{50}}}\right)^{\mathrm{X}}\right)$
3. $K_\mathrm{i} = \mathrm{IC_{50}}/(1 + [\mathrm{S}]/K_\mathrm{M})$
4. $[\mathrm{P}] = \frac{\mathrm{v_i} \times (1 - \exp(-k_\mathrm{obs}\mathrm{t}))}{k_\mathrm{obs}} + d$
5. $k_\mathrm{obs} = \frac{k_\mathrm{inac}}{K_\mathrm{i} \times (1 + [\mathrm{S}]/K_\mathrm{M})} \times [\mathrm{I}]$
6. $k_\mathrm{obs} = \frac{k_\mathrm{inac} \times [\mathrm{I}]}{K_\mathrm{i} \times (1 + [\mathrm{S}]/K_\mathrm{M}) + [\mathrm{I}]}$
7. $v = \frac{v_\mathrm{max} \times [\mathrm{S}]}{K_M + [S]}$

Figure 15: General equations.

Equation 1: Relative activity and IC_{50} calculation. IC_{50} is the half-maximal inhibitory concentration, [I] is the inhibitor concentration, v is the reaction rate in the presence of the inhibitor (%), v_0 is the reaction rate in the absence of the inhibitor (100 %).

Equation 2: Three-parameter equation. v is the reaction rate in the presence of the inhibitor (%), v_0 is the rate in absence of the inhibitor (100 %), IC_{50} is the half-maximal inhibitory concentration, [I] is the inhibitor concentration and x is a parameter for reaction stoichiometry.

Equation 3: Cheng-Prusoff equation. K_i is the inactivation constant, [S] is the substrate concentration and K_M is the Michaelis-Menten constant.

Equation 4: Non-linear regression and k_obs evaluation. [P] is the product concentration, v_i is the initial rate, k_obs is the observed first-order rate constant, t is time and d is the offset.

Equations 5 and 6: $k_\mathrm{inac}/K_\mathrm{i}$ evaluation. k_obs is the observed first-order rate constant, K_i is inactivation constant, [I] inhibitor concentration, [S] the substrate concentration and K_M the Michaelis-Menten constant.

Equation 7: Michaelis-Menten equation. v is the reaction rate, v_max is maximum velocity obtained at infinite substrate concentration, [S] is the substrate concentration and K_M is the Michaelis-Menten constant.

8 RESULTS

8.1 Imidazole compounds derived from *N*-protected cyclohexylalanine

First group of tested substances was synthesized by Jim Küppers, the member of prof. Gütschow's group. The imidazole core in these compounds replaces the carboxylic group of the benzyloxycarbonyl-protected cyclohexylalanine.

Five derivatives, in which the imidazole structure is once or twice substituted, were included to measurement. Double measurements of each tested compound in final concentration 5 μM did not show sufficient inhibition of cathepsins B, L, K and S. We set the limit for significant inhibition of 70 % of enzyme activity at a compound concentration of 5 μM. However, the HLE assays revealed interesting results for the evaluated compounds. Four out of five compounds **- 2573**, **3161**, **3162** and **3181** were identified as possible selective inhibitors for this enzyme. Because of the inhibitory potential on HLE, an additional serine protease - HT, was also investigated. No inhibition of HT was observed.

All five compounds showed problems with solubility at 5 μM under the original HLE assay conditions. Therefore, the final DMSO concentration was increased from 1.5 % to 2.5 %. Under these conditions, inhibitory potential of those four compounds was discovered. But modifying the assay conditions led to the need for determining a new K_M value as described below (page 35).

In addition to solubility problems, all measured substances showed also some kind of instability during the stock solution preparation. Plastic Eppendorf tubes should not be used for preparation because of a possible adsorption of compounds at the surface leading to the subsequent loss of inhibitory activity. Even when dark brown glass vials were used a slight loss of activity was observed, so it is always necessary to prepare fresh solutions. With regard to the chemical structure, chemical decomposition is not assumed, but rather some physical instability, such as adsorption to a particular surface as mentioned. The results are given below in Table 3.

Table 3: Enzyme inhibition by imidazole compounds derived from *N*-protected cyclohexylalanine.

№	Formula	Enzyme activity in presence of at 5 µM inhibitor (%)[a]					
		cat L	cat B	cat K	cat S	HLE	HT
2573	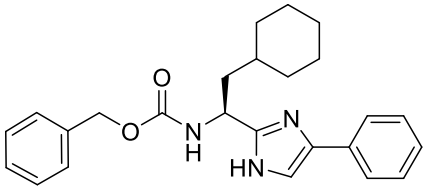 $C_{25}H_{29}N_3O_2$	94	100	70	91	< 20[b]	100
3161	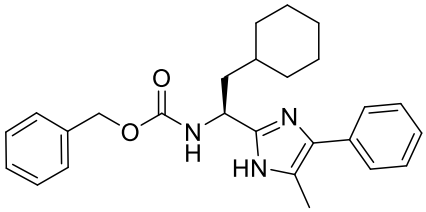 $C_{26}H_{31}N_3O_2$	89	99	74[c]	89	< 20[b]	103
3162	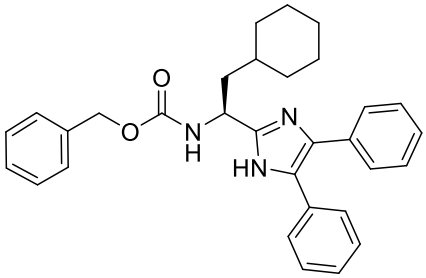 $C_{31}H_{33}N_3O_2$	89	97	95	91	< 20[b]	102
3181	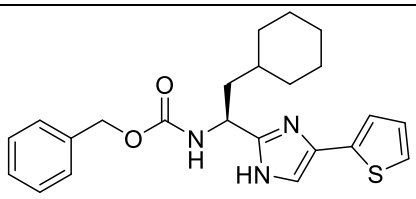 $C_{23}H_{27}N_3O_2S$	89	89	97	96	< 20[b]	99
3182	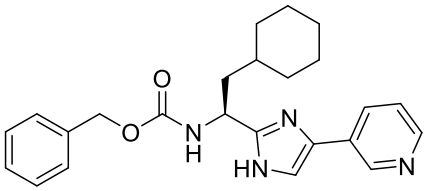 $C_{24}H_{28}N_4O_2$	97	92	104	91	101	98

For footnote, see the next page.

[a] All measurements were performed in duplicates. Cathepsin B (cat B), cathepsin L (cat L), cathepsin K (cat K) and cathepsin S (cat S) were assayed over 60 min. Human leukocyte elastase (HLE) and human thrombin (HT) assays were followed over 10 min. Differences between absorbances or fluorescences at the beginning and at the end of the assay were used for determination of the final product concentration. The values of the control reactions were set to 100 %.

[b] Enzyme activity lower than 20 % was designated as a limit for subsequent concentration-dependent measurements.

[c] Reactions were measured in duplicates using two different concentrations (6 μM, 9 μM) of the inhibitor. Enzyme activity at 5 μM of the compound was calculated from data obtained at the applied concentration according to the equation 1 (Figure 15, page 38).

Because compounds **2573**, **3161**, **3162** and **3181** at 5 μM caused the HLE activity of less than 20 %, concentration-dependent measurements were performed. 10 different concentrations of each tested compound were investigated. Since the 10 min progress curves were linear, compounds can be considered as reversible inhibitors. The relative activity was calculated from linear evaluation at each concentration according to the equation 1 (Figure 15, page 38). Non-linear three-parameter regression according to the equation 2 (Figure 15, page 38) was used for determination of IC_{50} values. The same analysis was used in the study focused on inhibition of HLE by Brunsvicamides A-C.[38] Parameter x indicates an imbalance in the reaction stoichiometry. Therefore, the enzyme and the substrate do not react together in a proportion 1:1, but there is probably some other interaction in the reaction. Our data were also analyzed by non-liner regression using a two-parameter equation, where parameter x equals 1, but our data did not fit so much in this equation. To consider assay conditions and to get more comparable results, IC_{50} values were related by the factor containing K_M and substrate concentration.

The results obtained by both methods are included in Table 4. Three compounds, **3161, 3162** and **3181**, were identified as selective reversible inhibitors for HLE with $IC_{50} < 2.5$ μM. The progress curves showed a time- and concentration-dependent reversible inhibition. The compound **3161** ($IC_{50}/(1 + [S]/K_M) = 0.60 \pm 0.03$ μM), where the imidazole ring is substituted with methyl and phenyl, was identified as the best selective inhibitor of HLE out of this series of compounds. The imidazole derivate

with two phenyl substituents **3162** ($IC_{50}/(1+[S]/K_M)$ = 0.96 ± 0.06 µM) and the thienyl-substituted **3181** ($IC_{50}/(1+[S]/K_M)$ = 1.16 ± 0.02 µM) showed a somewhat weaker inhibitory potency towards the HLE. Compound **2573**, where the imidazole is substituted by one phenyl residue, showed insufficient inhibition characterized by IC_{50} > 2.5 µM. For **3182**, inhibition was not observed. Because of compound **3182**, imidazole compounds derived from *N*-protected cyclohexylalanine cannot be generally considered as inhibitors of HLE. Graphs and detailed summary of the individual inhibitors with IC_{50} < 2.5 µM are given below in Figures 16, 17, 18.

Table 4: Human leukocyte elastase inhibition by promising compounds **2573**, **3161**, **3162**, **3181**.[a]

№	Three-parameters model			Two-parameters model		
	IC_{50} (µM)	x	$\frac{IC_{50}}{\left(1+\frac{[S]}{K_M}\right)}$	IC_{50} (µM)	x	$\frac{IC_{50}}{\left(1+\frac{[S]}{K_M}\right)}$
2573	3.02 ± 0.06	9.33 ± 1.98	1.55 ± 0.03	7.18 ± 2.92	1	3.66 ± 1.49
3161	1.18 ± 0.06	2.69 ± 0.27	0.60 ± 0.03	0.71 ± 0.20	1	0.36 ± 0.10
3162	1.88 ± 0.12	3.76 ± 0.75	0.96 ± 0.06	1.37 ± 0.48	1	0.70 ± 0.24
3181	2.27 ± 0.04	5.05 ± 0-47	1.16 ± 0.02	2.21 ± 0.84	1	1.13 ± 0.84

[a] 10 different concentrations of compounds were measured once every 10 minutes and values of the half-maximal inhibitory concentration (IC_{50}) were evaluated by non-linear regression with two- and three-parameters model according to the equation 2 (Figure 15, page 38). [S] is the substrate concentration and K_M is the Michaelis-Menten constant.

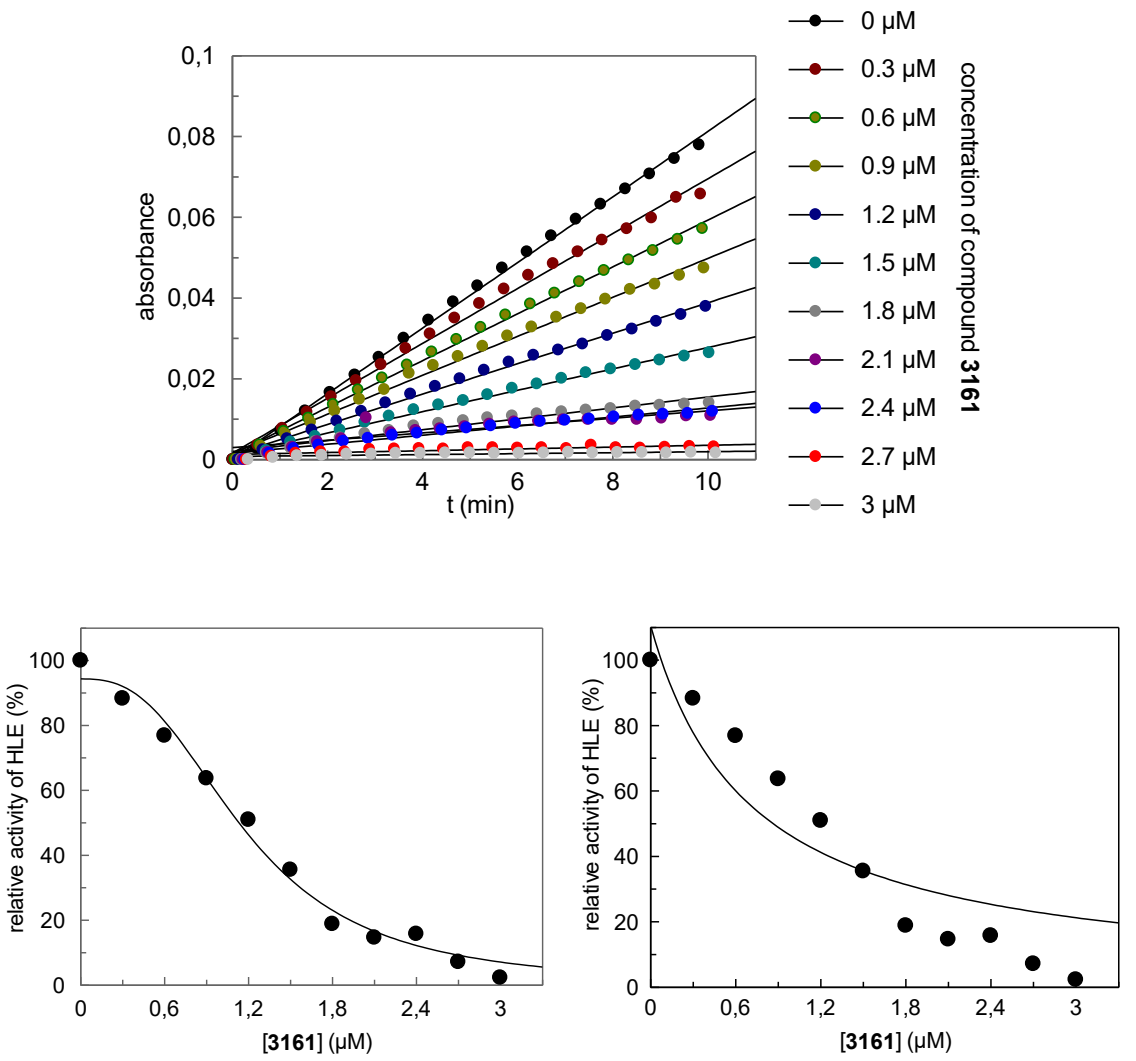

Figure 16: Inhibition of human leukocyte elastase by compound **3161**.

The substrate concentration was 100 µM (0.96 K_M) Upper: Product formation in the presence of different inhibitor concentrations. The progress curves were analyzed by linear regression. Lower: The relative activities were plotted against the inhibitor concentrations. Lower left: The half-maximal inhibitory concentration (IC_{50}) of 1.18 ± 0.06 µM was obtained by non-linear regression using the equation 2 (Figure 15, page 38), where x = 2.69 ± 0.27. Lower right: An IC_{50} value of 0.71 ± 0.20 µM was obtained by non-linear regression using the same equation (x = 1). Graphs and kinetic evaluation were made by the author of the thesis in GraFit - data analysis software for Windows.

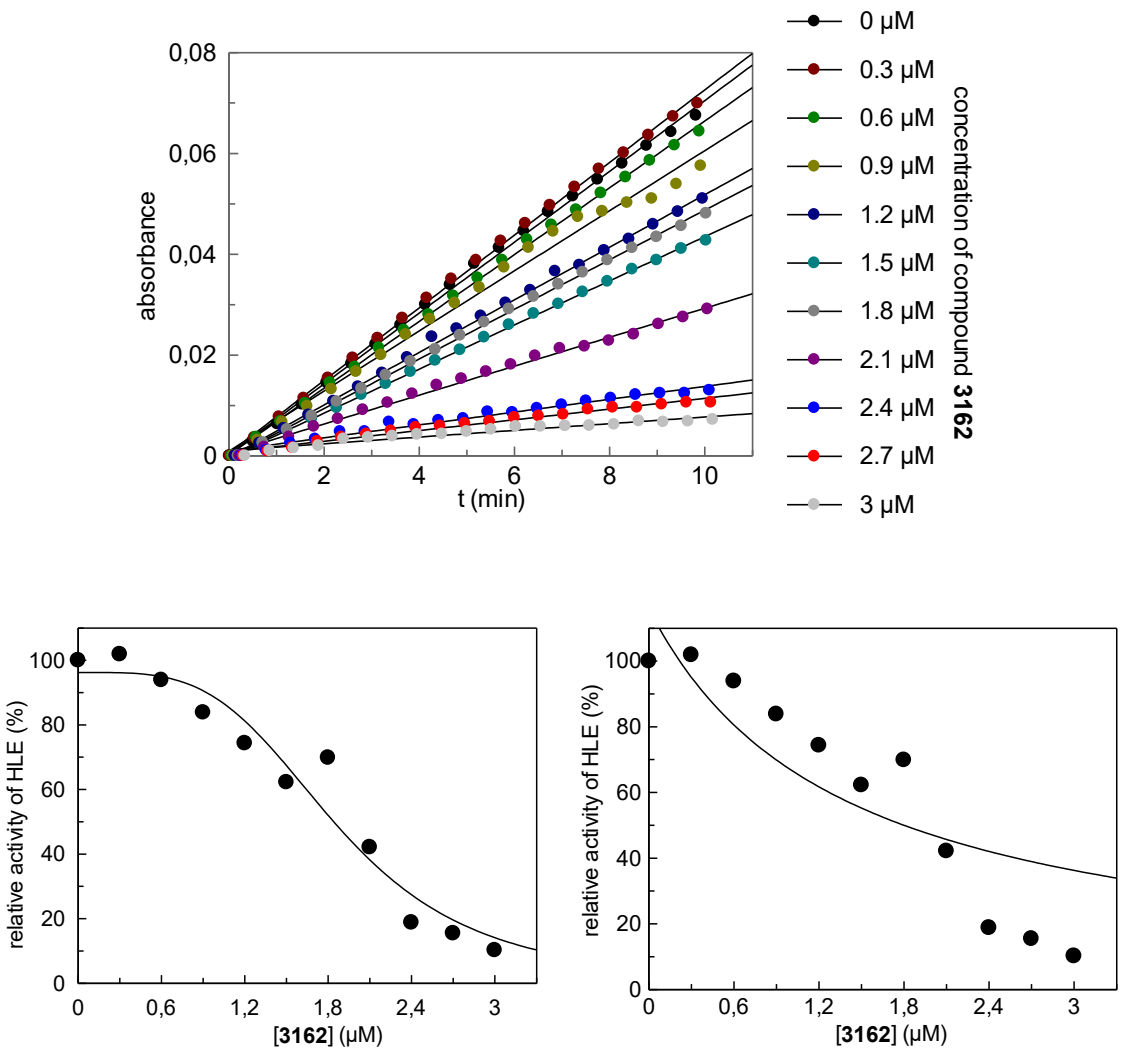

Figure 17: Inhibition of human leukocyte elastase by compound **3162**.

The substrate concentration was 100 µM (0.96 K_M). Upper: Product formation in the presence of different inhibitor concentrations. The progress curves were analyzed by linear regression. Lower: The relative activities were plotted against the inhibitor concentrations. Lower left: The half-maximal inhibitory concentration (IC_{50}) of 1.88 ± 0.12 µM was obtained by non-linear regression using the equation 2 (Figure 15, page 38), where x = 3.76 ± 0.75. Lower right: An IC_{50} value of 1.37 ± 0.48 µM was obtained by non-linear regression using the same equation (x = 1). Graphs and kinetic evaluation were made by the author of the thesis in GraFit - data analysis software for Windows.

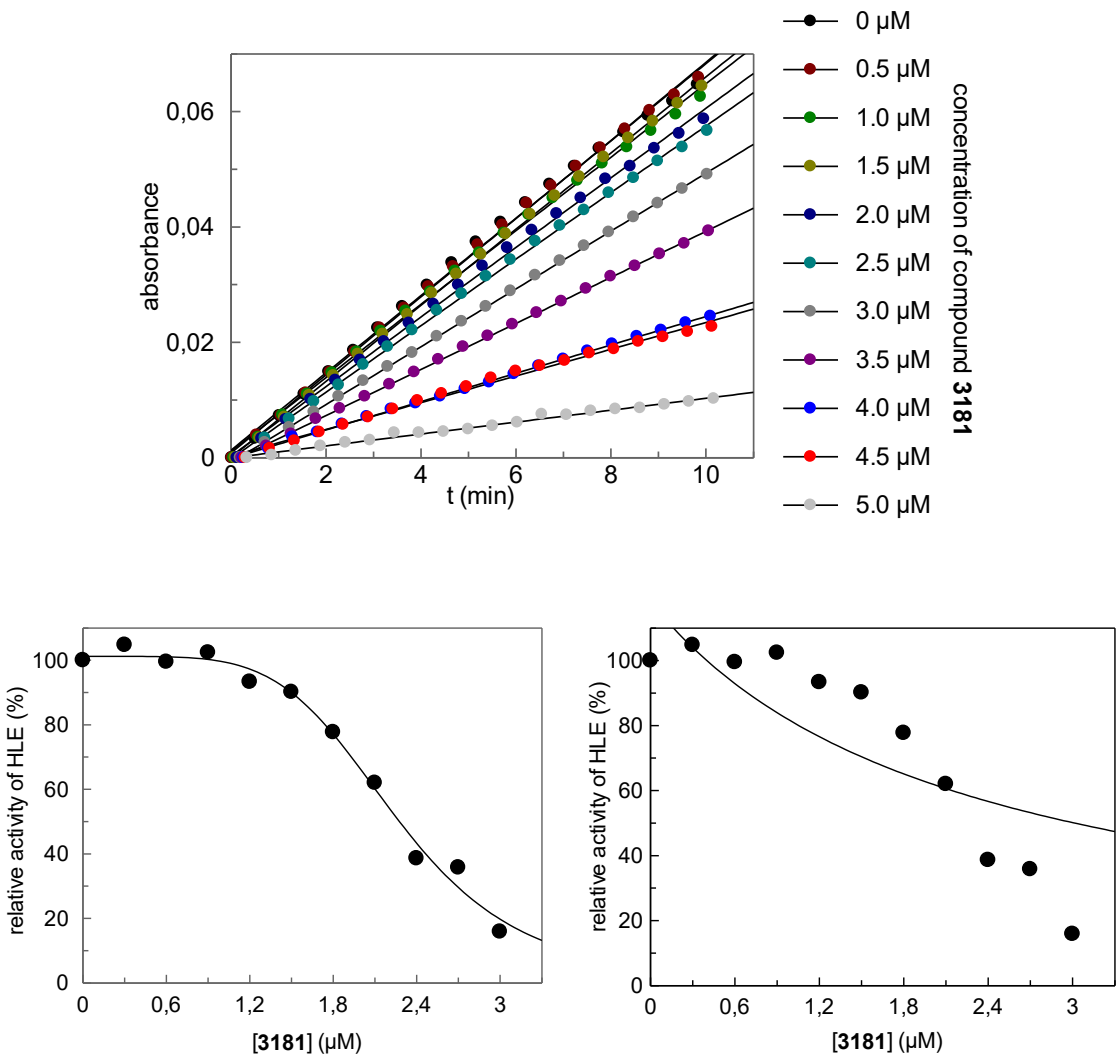

Figure 18: Inhibition of human leukocyte elastase by compound **3181**.

The substrate concentration was 100 µM (0.96 K_M) Upper: Product formation in the presence of different inhibitor concentrations. The progress curves were analyzed by linear regression. Lower: The relative activities were plotted against the inhibitor concentrations. Lower left: The half-maximal inhibitory concentration (IC_{50}) of 2.27 ± 0.04 µM was obtained by non-linear regression using the equation 2 (Figure 15, page 38), where x = 5.05 ± 0.47. Lower right: An IC_{50} value of 2.21 ± 0.84 µM was obtained by non-linear regression using the same equation (x = 1). Graphs and kinetic evaluation were made by the author of the thesis in GraFit - data analysis software for Windows.

8.2 2-Phenyl-7,8-dihydroimidazo[1,2-*a*]pyrazin-6(5*H*)one derivatives

Other group of tested substances were synthesized by Jim Küppers as well. The main structure of this group belongs to compound **3173**, 2-phenyl-7,8-dihydroimidazo[1,2-*a*]pyrazin-6(5*H*)one. Other compounds are substituted at position 8. Exception is compound **3178**, where pyrazine has one more carbon added in the ring. Just like the previous group, these compounds were at first tested on cathepsins and HLE. None of the tested substances at concentration 5 μM has shown any inhibitory potency against the assayed enzymes. Further testing was not performed. All experiments were conducted without any problems with stability or solubility. The results are given below in Table 5.

Table 5: Enzyme inhibition by derivatives of 2-phenyl-7,8-dihydroimidazo[1,2-a]pyrazin-6(5*H*)one.

№	Formula	Enzyme activity at 5 μM (%)[a]				
		cat L	cat B	cat K	cat S	HLE
2579	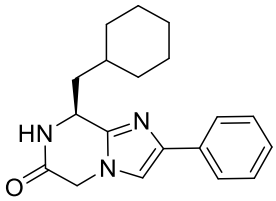 $C_{19}H_{23}N_3O$	98	101	79	88	104
3172	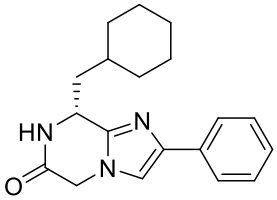 $C_{19}H_{23}N_3O$	96	96	73	88	100
3173	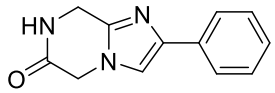 $C_{12}H_{11}N_3O$	100	98	89	84	97
3174	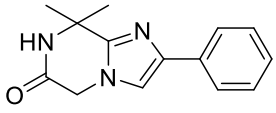 $C_{14}H_{15}N_3O$	99	96	97	86	104

Table 5: Continuation

3175	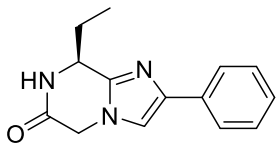 $C_{14}H_{15}N_3O$	97	99	93	93	101
3176	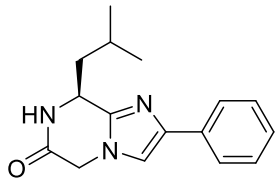 $C_{16}H_{19}N_3O$	98	96	86	86	100
3177	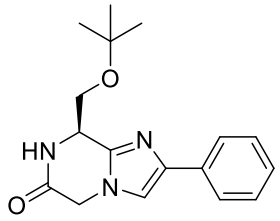 $C_{17}H_{21}N_3O_2$	99	96	89	81	95
3178	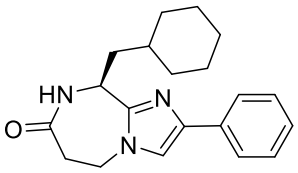 $C_{20}H_{25}N_3O$	98	95	88	89	94
3179	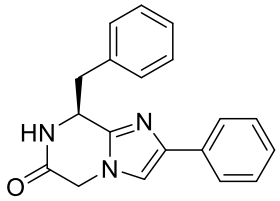 $C_{19}H_{17}N_3O$	97	95	89	86	94

[a] All measurements were performed in duplicates at the compound concentration of 5 µM. Cathepsin B (cat B), cathepsin L (cat L), cathepsin K (cat K) and cathepsin S (cat S) were assayed over 60 min. Human leukocyte elastase (HLE) inhibition assays were followed over 10 min. Differences between absorbances or fluorescences at the beginning and at the end of the assay were used for determination of the final product concentration. The values of the control reactions were set to 100 %.

8.3 α,β-Unsaturated peptidomimetic compounds

The next tested compounds were synthesized by other member of our group, Christian Breuer. The main structural feature of this group is an α,β-unsaturated carbonyl moiety integrated into a peptide structure. These compounds were synthesized as potential cat B inhibitors. Therefore, they were tested only on cathepsins. The results have not shown any significant inhibition (Table 6).

Table 6: Enzyme inhibition by α,β-unsaturated peptidomimetic compounds

№	Formula	C (μM)	Enzyme activity (%)[a]			
			cat L	cat B	cat K	cat S
3163	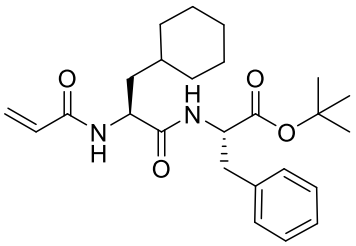 $C_{25}H_{36}N_2O_4$	5	97	93	75[b]	93[b]
		10	97	96	67[b]	84[b]
		20	93	89	59[b]	83[b]
3169	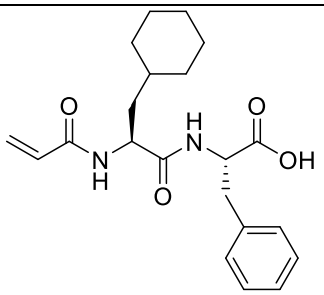 $C_{21}H_{28}N_2O_4$	5	98	98	89	95
		10	95	95	78	90
		20	97	87	78	84
3170	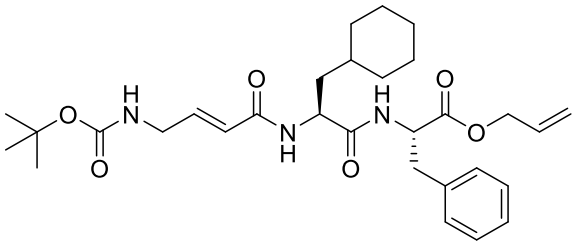 $C_{30}H_{43}N_3O_6$	5	88	89	89	81
		10	95	94	87	66
		20	90	92	74	60

For footnote, see the next page.

[a] All measurements with cathepsin B (cat B), cathepsin L (cat L), cathepsin K (cat K) and cathepsin S (cat S) were performed in duplicates at the compound concentration of 5, 10 and 20 µM. Reactions were followed over 60 min. Differences between absorbances or fluorescences at the beginning and at the end of the assay were used for determination of the final product concentration. The values of the control reactions were set to 100 %.

[b] The measurements shown here were performed by Carina Lemke.

8.4 Carbamate

The chemotype of peptidic carbamate inhibitors has been developed in the prof. Gütschow's group as irreversible inhibitors of cysteine proteases, in particular cat B. Carbamate **3167** was synthesized by Jim Küppers. In the course of this thesis, inhibitory activity of synthesized compound was investigated on cat B. Further enzyme assays will be performed by other group members. The compound at the concentration of 20 µM, decreased the enzyme activity to 66 %. Concentration-dependent measurement at 5 different concentrations was performed. From the obtained values, compound **3167** can be considered as an irreversible cat B inhibitor. Results are given in Table 7 and Figure 19.

Table 7: Cathepsin B inhibition by compound **3167**.

№	Formula	Enzyme activity (%)[a]	$k_{inac}/K_i \pm$ S.E. (µM)[b]
3167	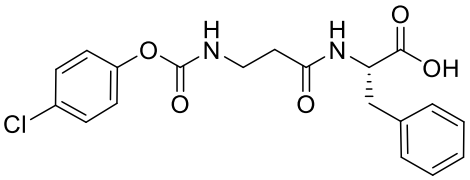 $C_{19}H_{19}ClN_2O_5$	66	12.44 ± 0.49

[a] Measurement was performed duplicates at 20 µM compound concentration. Reaction was followed over 60 min. Differences between absorbances or fluorescences at the beginning and at the end of the assay were used for determination of the final product concentration. The values of the control reactions were set to 100 %.

[b] Sample was measured in duplicates at inhibitor concentration of 10, 20, 30, 40 and 50 µM. Observed first-order rate constant (k_{obs}) values calculated according to the

equation 5 (Figure 15, page 38) were plotted against the inhibitor concentration. The second order rate parameter (k_{inac}/K_i) was determined by the equation 6 (Figure 15, page 38). S.E. is a standard error. The substrate concentration was 500 µM (0.45 K_M).[35]

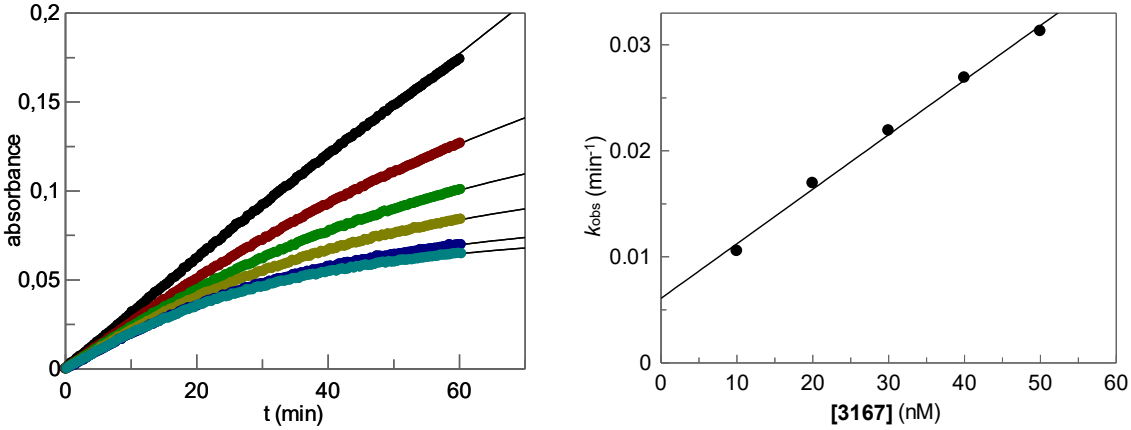

Figure 19: Inhibition of human cathepsin B by **3167**.

Left: Product formation in the presence of different inhibitor concentrations. From the top to the bottom: 0 µM (black line), 10 µM (red line), 20 µM (green line), 30 µM (dark yellow line), 40 µM (dark blue line), 50 µM (light blue line). The progress curves were analyzed by nonlinear regression. Right: The observed first-order rate constant (k_{obs}) from duplicate measurements were plotted against the inhibitor concentrations [I]. A k_{obs}/[I] value of 8.58 ± 0.34 µM^{-1}s^{-1} was obtained by linear regression according to the equation 5 (Figure 15, page 38). The second order rate parameter (k_{inac}/K_i) of 12.44 ± 0.49 µM^{-1}s^{-1} was obtained. Kinetic evaluation and graphs were made by the author of the thesis in GraFit - data analysis software for Windows.

8.5 *N,N*-dibenzylcrotonamide derivative

Compound **3110**, an *N,N*-dibenzylcrotonamide derivative, was synthesized by Christian Breuer as potential cat K inhibitor. It contains an α,β-unsaturated Michael acceptor substructure again, which is investigated as a moiety useful for cathepsin inhibition.[41] Only concentration-dependent measurements at cat K were performed in the course of this thesis. Further enzyme assays will be performed by other group members. Data were obtained from the cat K inhibition assay, which indicate compound **3110** to be an irreversible cat K inhibitor. The result can be seen in **Table 8** and in Figure 20.

Table 8: Cathepsin K inhibition by compound **3110**.[a]

№	Formula	k_{inac}/K_i ± S.E. (μM)[b]	k_{inac}/K_i ± S.E. (μM)[c]
3110	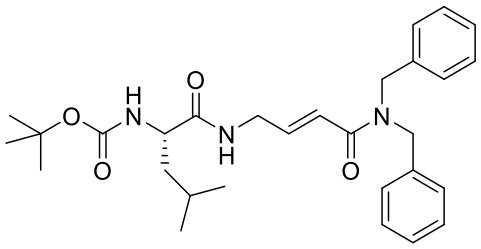	2293 ± 241	5940 ± 1717

[a] Measurements were performed in duplicates at the compound concentrations of 1, 2, 3, 4, 5 μM. Reactions were followed over 60 min. The observed first-order rate constant (k_{obs}) values from product progress curves were plotted against the inhibitor concentration. The substrate concentration was 40 μM (3.01 K_M).[35]

[b] The second order rate parameter (k_{inac}/K_i) was obtained by linear regression according to the equation 5 (Figure 15, page 38). S.E. is a standard error.

[c] k_{inac}/K_i was obtained by non-linear regression, according to the equation 6 (Figure 15, page 38).

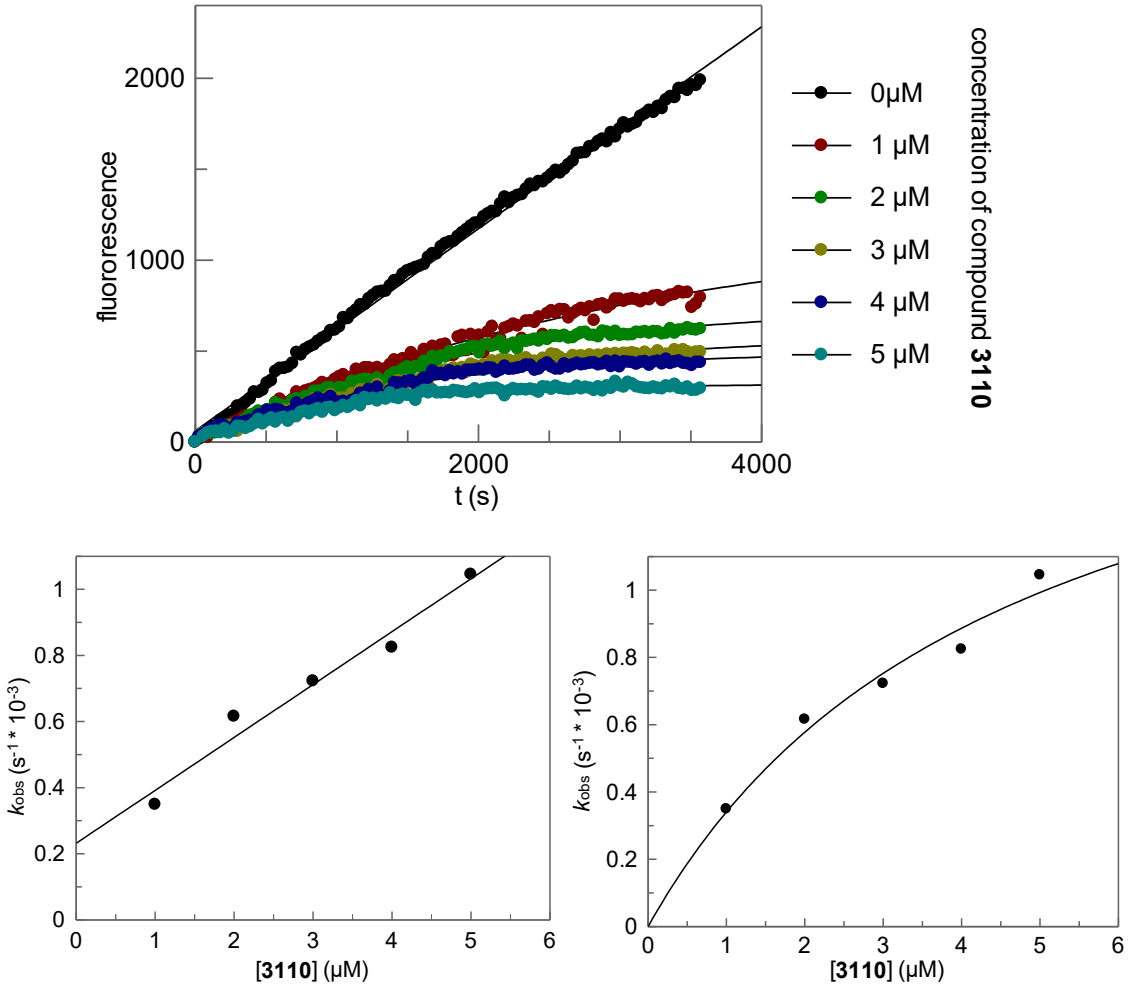

Figure 20: Inhibition of human cathepsin K by **3110**.

Upper: Product formation in the presence of different inhibitor concentrations. The progress curves analyzed by nonlinear regression indicate irreversible inhibition. Lower: The observed first-order rate constant (k_{obs}) from duplicate measurements were plotted against the inhibitor concentrations [I]. Lower left: A k_{obs}/[I] value of 160.0 ± 16.8 µM was obtained according to the equation 4 (Figure 15, page 38). The second order rate parameter (k_{inac}/K_i) of 2293 ± 241 was calculated according to the equation 5 (Figure 15, page 38). Lower right: A k_{obs}/[I] value of 414.5 ± 119.8 µM was analyzed by non-linear regression according to the equation 5 (Figure 15, page 38). The k_{inac}/K_i value of 5940 ± 1717 was calculated according to the equation 6 (Figure 15, page 38). Kinetic evaluation and graphs were made by the author of the thesis in GraFit - data analysis software for Windows.

8.6 Peptoides

The peptoides synthesized by Franziska Kohl represent the last tested group of compounds included in this thesis. A set of six peptoides, poly-*N*-substituted glycines, were tested only at cat L. No inhibition was observed. The obtained values are included below in Table 9.

Table 9: Cathepsin L inhibition by peptoides.

№	Formula	cat L activity (%)[a]	№	Formula	cat L activity (%)[a]
FK-3E5	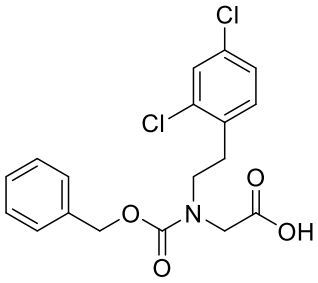	94	**FK-1NBoc**	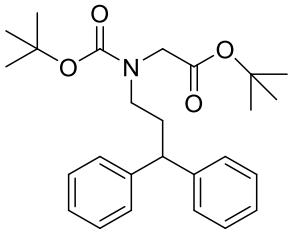	90
FK-1H	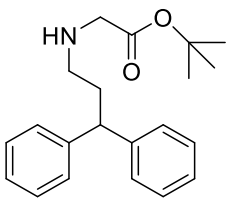	96	**FK-1PhEs**	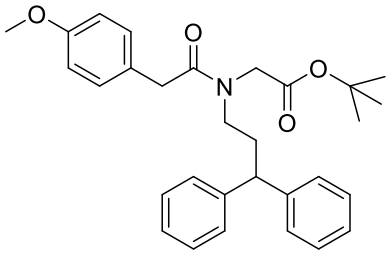	97
FK-7E	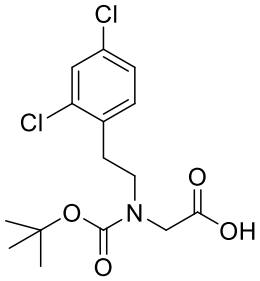	98	**JS 354**	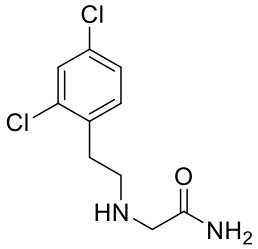	99

[a] All measurements with cathepsin L (cat L) were performed in duplicates at the peptoide concentration of 1 µM. Reactions were followed over 60 min. Differences between absorbances or fluorescences at the beginning and at the end of the assay were used for determination of the final product concentration. The values of the control reactions were set to 100 %.

9 DISCUSSION

In this diploma thesis, there is presented the enzyme inhibition activity of new potential inhibitors against human cathepsins B, L, S, K, which belong to cysteine proteases, as well as against representatives of serine proteases, HLE and HT.

The imidazole compounds derived from *N*-protected cyclohexylalanine were synthesized and their inhibitory potential was unknown. During the investigation, a reversible inhibition of HLE was observed. The non-covalent inactivation and the concentration-dependent inhibition were concluded from linear progress curves. As a sign of selectivity, the compounds did not demonstrate inhibition of tested cathepsins and HT. All measured substances showed some kind of instability during the stock solution preparation. Plastic Eppendorf tubes should not be used for storage of the compounds' solution, because of subsequent loss of inhibitory activity. Even when dark brown glass vials were used, a slight loss of activity was observed. So it was always necessary to prepare fresh solutions. With regard to the chemical structure, chemical decomposition is not assumed, but rather some physical instability, such as adsorption to a particular surface. The compounds also showed problems with solubility at 5 μM under the original HLE assay conditions. Therefore, the final DMSO concentration was increased (from 1.5 % to 2.5 %) and a new K_M value was determined. The best inhibitor was compound **3161** containing the imidazole substituted by methyl and phenyl residues ($IC_{50}/(1 + [S]/K_M)$ = 0.60 ± 0.03 μM). The other compounds from this group also act as reversible inhibitors, except for compound **3182**. There was no inhibition observed. Because of this last compound, the general inhibitory potential of this group cannot be concluded. But some similar derivatives should be prepared and investigated in the future.

The 2-phenyl-7,8-dihydroimidazo[1,2-*a*]pyrazin-6(5*H*)-one compounds were also synthesized with unknown inhibitory potential. In this case, inhibition was not observed. The bicyclic structure containing the imidazole seems to be less appropriate for HLE inhibition than the monocyclic imidazole moiety in the previous group.

The irreversible inhibition of cysteine proteases was expected for the α,β-unsaturated peptidomimetic compounds, based on their Michael acceptor substructure.[41] But the inhibition of cathepsins B, L, K and S by this group of compounds was not observed.

Compounds containing the carbamate structure have been developed in the prof. Gütschow's group as irreversible inhibitors of cysteine proteases. In the literature, similar compounds can be found, which are inhibiting some cysteine cathepsins.[42–44] In the course of this thesis, carbamate **3167** was investigated as potential cat B inhibitor. Kinetic evaluation demonstrated the concentration-dependent activity, where non-linear progress curves and k_{inac}/K_i value of 12.44 ± 0.49 $\mu M^{-1}s^{-1}$ were observed. From these results, this compound can be considered as an irreversible inhibitor of cat B. The data also confirm carbamate derivatives as a promising approach for the cysteine inhibitor development.

The *N,N*-dibenzylcrotonamide derivative also contains an α,β-unsaturated Michael acceptor substructure, as in case of the α,β-unsaturated peptidomimetic compounds. The inhibitory activity of compound **3110** belonging to this group was investigated on cat K. The observation of concentration-dependent measurement with non-linear progress curves and the k_{inac}/K_i value of 2293 ± 241 $\mu M^{-1}s^{-1}$ supports the irreversible inhibition. The results also confirm Michael acceptors as an appropriate substructure in the cysteine inhibitor development.

The peptoides were synthesized and their inhibitory potential was unknown. Their investigation did not show any inhibitory potency against cat L.

10 CONCLUSION

In summary, some potent inhibitors have been found. In case of imidazole derivatives, four compounds have been characterized as reversible inhibitors. The compound **3167** has shown that the use of the carbamate structure is a useful approach in development of cat B inhibitors. But because only one carbamate compound was included in this project, it is necessary to evaluate more carbamate-type compounds for extended conclusions. The *N,N*-dibenzylcrotonamide derivative (**3110**) as observed cat K inhibitor offers possibilities of Michael acceptor elements within the structures of the irreversible cat K inhibitors. Further representatives of this chemotype need to be investigated in the future.

11 LIST OF FIGURES AND TABLES

12 REFERENCES

1. Turk, V., Stoka, V., Vasiljeva, O., Renko, M., Sun, T., Turk, B. & Turk, D. Cysteine cathepsins: from structure, function and regulation to new frontiers. *Biochim. Biophys. Acta* **1824,** 68–88 (2012).
2. Hedstrom, L. Serine protease mechanism and specificity. *Chem. Rev.* **102,** 4501–4524 (2002).
3. Zerbini, C. A. F. & McClung, M. R. Odanacatib in postmenopausal women with low bone mineral density: a review of current clinical evidence. *Ther. Adv. Musculoskelet. Dis.* **5,** 199–209 (2013).
4. Aikawa, N., Ishizaka, A., Hirasawa, H., Shimazaki, S., Yamamoto, Y., Sugimoto, H., Shinozaki, M., Taenaka, N., Endo, S., Ikeda, T. & Kawasaki, Y. Reevaluation of the efficacy and safety of the neutrophil elastase inhibitor, Sivelestat, for the treatment of acute lung injury associated with systemic inflammatory response syndrome; a phase IV study. *Pulm. Pharmacol. Ther.* **24,** 549–554 (2011).
5. Siklos, M., BenAissa, M. & Thatcher, G. R. J. Cysteine proteases as therapeutic targets: does selectivity matter? A systematic review of calpain and cathepsin inhibitors. *Acta Pharm. Sin. B* **5,** 506–519 (2015).
6. Kos, J., Mitrović, A. & Mirković, B. The current stage of cathepsin B inhibitors as potential anticancer agents. *Future Med. Chem.* **6,** 1355–1371 (2014).
7. Ekici, O. D., Paetzel, M. & Dalbey, R. E. Unconventional serine proteases: variations on the catalytic Ser/His/Asp triad configuration. *Protein Sci.* **17,** 2023–2037 (2008).
8. Schechter, I. & Berger, A. On the size of the active site in proteases. I. Papain. *Biochem. Biophys. Res. Commun.* **27,** 157–162 (1967).
9. Lecaille, F., Kaleta, J. & Brömme, D. Human and parasitic papain-like cysteine proteases: their role in physiology and pathology and recent developments in inhibitor design. *Chem. Rev.* **102,** 4459–4488 (2002).
10. Löser, R. & Pietzsch, J. Cysteine cathepsins: their role in tumor progression and recent trends in the development of imaging probes. *Front. Chem.* **3,** 37 (2015).
11. Wilkinson, R. D. A., Williams, R., Scott, C. J. & Burden, R. E. Cathepsin S: therapeutic, diagnostic, and prognostic potential. *Biol. Chem.* **396,** 867–882 (2015).

12. Fonović, M. & Turk, B. Cysteine cathepsins and extracellular matrix degradation. *Biochim. Biophys. Acta* **1840,** 2560–2570 (2014).
13. Erez, E., Fass, D. & Bibi, E. How intramembrane proteases bury hydrolytic reactions in the membrane. *Nature* **459,** 371 (2009).
14. von Nussbaum, F. & Li, V. M.-J. Neutrophil elastase inhibitors for the treatment of (cardio)pulmonary diseases: Into clinical testing with pre-adaptive pharmacophores. *Bioorg. Med. Chem. Lett.* **25,** 4370–4381 (2015)
15. Sjö, P. Neutrophil elastase inhibitors: recent advances in the development of mechanism-based and nonelectrophilic inhibitors. *Future Med. Chem.* **4,** 651–660 (2012).
16. Licari, L. G. & Kovacic, J. P. Thrombin physiology and pathophysiology. *J. Vet. Emerg. Crit. Care San Antonio* **19,** 11–22 (2009).
17. Arsenault, K. A., Hirsh, J., Whitlock, R. P. & Eikelboom, J. W. Direct thrombin inhibitors in cardiovascular disease. *Nat. Rev. Cardiol.* **9,** 402–414 (2012).
18. Lee, C. J. & Ansell, J. E. Direct thrombin inhibitors. *Br. J. Clin. Pharmacol.* **72,** 581–592 (2011).
19. Copeland, R. A. Evaluation of enzyme inhibitors in drug discovery. A guide for medicinal chemists and pharmacologists. *Methods Biochem. Anal.* **46,** 1–265 (2005).
20. Vergelli, C., Schepetkin, I. A., Crocetti, L., Iacovone, A., Giovannoni, M. P., Guerrini, G., Khlebnikov, A. I., Ciattini, S., Ciciani, G. & Quinn, M. T. Isoxazol-5(2H)-one: a new scaffold for potent human neutrophil elastase (HNE) inhibitors. *J. Enzyme Inhib. Med. Chem.* **32,** 821–831 (2017).
21. Crocetti, L., Bartolucci, G., Cilibrizzi, A., Giovannoni, M. P., Guerrini, G., Iacovone, A., Menicatti, M., Schepetkin, I. A., Khlebnikov, A. I., Quinn, M. T. & Vergelli, C. Synthesis and analytical characterization of new thiazol-2-(3H)-ones as human neutrophil elastase (HNE) inhibitors. *Chem. Cent. J.* **11,** 127 (2017).
22. Brömme, D. & Lecaille, F. Cathepsin K inhibitors for osteoporosis and potential off-target effects. *Expert Opin. Investig. Drugs* **18,** 585–600 (2009).
23. Balicatib. at <https://www.drugbank.ca/drugs/DB12239> [cit. 10.1.2018]

24. Costa, A. G., Cusano, N. E., Silva, B. C., Cremers, S. & Bilezikian, J. P. Cathepsin K: its skeletal actions and role as a therapeutic target in osteoporosis. *Nat. Rev. Rheumatol.* **7,** 447–456 (2011).

25. Mukherjee, K. & Chattopadhyay, N. Pharmacological inhibition of cathepsin K: A promising novel approach for postmenopausal osteoporosis therapy. *Biochem. Pharmacol.* **117,** 10–19 (2016).

26. Yasuda, Y., Kaleta, J. & Brömme, D. The role of cathepsins in osteoporosis and arthritis: rationale for the design of new therapeutics. *Adv. Drug Deliv. Rev.* **57,** 973–993 (2005).

27. Bone, H. G., McClung, M. R., Roux, C., Recker, R. R., Eisman, J. A., Verbruggen, N., Hustad, C. M., DaSilva, C., Santora, A. C. & Ince, B. A. Odanacatib, a cathepsin-K inhibitor for osteoporosis: a two-year study in postmenopausal women with low bone density. *J. Bone Miner. Res.* **25,** 937–947 (2010).

28. Eisman, J. A., Bone, H. G., Hosking, D. J., McClung, M. R., Reid, I. R., Rizzoli, R., Resch, H., Verbruggen, N., Hustad, C. M., DaSilva, C., Petrovic, R., Santora, A. C., Ince, B. A. & Lombardi, A. Odanacatib in the treatment of postmenopausal women with low bone mineral density: three-year continued therapy and resolution of effect. *J. Bone Miner. Res.* **26,** 242–251 (2011).

29. Langdahl, B., Binkley, N., Bone, H., Gilchrist, N., Resch, H., Rodriguez Portales, J., Denker, A., Lombardi, A., Le Bailly De Tilleghem, C., Dasilva, C., Rosenberg, E. & Leung, A. Odanacatib in the treatment of postmenopausal women with low bone mineral density: five years of continued therapy in a phase 2 study. *J. Bone Miner. Res.* **27,** 2251–2258 (2012).

30. Rizzoli, R., Benhamou, C.-L., Halse, J., Miller, P. D., Reid, I. R., Rodríguez Portales, J. A., DaSilva, C., Kroon, R., Verbruggen, N., Leung, A. T. & Gurner, D. Continuous treatment with odanacatib for up to 8 years in postmenopausal women with low bone mineral density: a phase 2 study. *Osteoporos. Int.* **27,** 2099–2107 (2016).

31. Engelke, K., Fuerst, T., Dardzinski, B., Kornak, J., Ather, S., Genant, H. K. & de Papp, A. Odanacatib treatment affects trabecular and cortical bone in the femur

of postmenopausal women: results of a two-year placebo-controlled trial. *J. Bone Miner. Res.* **30,** 30–38 (2015).

32. Bone, H. G., Dempster, D. W., Eisman, J. A., Greenspan, S. L., McClung, M. R., Nakamura, T., Papapoulos, S., Shih, W. J., Rybak-Feiglin, A., Santora, A. C., Verbruggen, N., Leung, A. T. & Lombardi, A. Odanacatib for the treatment of postmenopausal osteoporosis: development history and design and participant characteristics of LOFT, the Long-Term Odanacatib Fracture Trial. *Osteoporos. Int.* **26,** 699–712 (2015).
33. Merck & Co., Inc. - Merck Provides Update on Odanacatib Development Program. at <http://investors.merck.com/news/press-release-details/2016/Merck-Provides-Update-on-Odanacatib-Development-Program/default.aspx> [cit. 20.2.2018]
34. Klinické hodnocení léků, Státní ústav pro kontrolu léčiv. at <http://www.sukl.cz/klinicke-hodnoceni-leku> [cit. 20.2.2018]
35. Frizler, M., Lohr, F., Furtmann, N., Kläs, J. & Gütschow, M. Structural optimization of azadipeptide nitriles strongly increases association rates and allows the development of selective cathepsin inhibitors. *J. Med. Chem.* **54,** 396–400 (2011).
36. Mertens, M. D., Schmitz, J., Horn, M., Furtmann, N., Bajorath, J., Mareš, M. & Gütschow, M. A coumarin-labeled vinyl sulfone as tripeptidomimetic activity-based probe for cysteine cathepsins. *Chembiochem* **15,** 955–959 (2014).
37. Dosa, S., Stirnberg, M., Lülsdorff, V., Häußler, D., Maurer, E. & Gütschow, M. Active site mapping of trypsin, thrombin and matriptase-2 by sulfamoyl benzamidines. *Bioorg. Med. Chem.* **20,** 6489–6505 (2012).
38. Sisay, M. T., Hautmann, S., Mehner, C., König, G. M., Bajorath, J. & Gütschow, M. Inhibition of human leukocyte elastase by brunsvicamides a-C: cyanobacterial cyclic peptides. *ChemMedChem* **4,** 1425–1429 (2009).
39. Gütschow, M. *personal communication: personal communication.*
40. Schmitz, J. Synthesis and Biological Evaluation of Nitrile-Based Peptidomimetic Inhibitors for Cysteine Cathepsins. *Dissertation* (2016), prof

Gütschow group, department of pharmaceutical chemistry, Rheinische Friedrich-Wilhelms-Universität Bonn, Germany.

41. Santos, M. M. M. & Moreira, R. Michael acceptors as cysteine protease inhibitors. *Mini Rev. Med. Chem.* **7,** 1040–1050 (2007).

42. Epple, R., Urbina, H. D., Russo, R., Liu, H., Mason, D., Bursulaya, B., Tumanut, C., Li, J. & Harris, J. L. Bicyclic carbamates as inhibitors of papain-like cathepsin proteases. *Bioorg. Med. Chem. Lett.* **17,** 1254–1259 (2007).

43. Ghosh, A. K. & Brindisi, M. Organic carbamates in drug design and medicinal chemistry. *J. Med. Chem.* **58,** 2895–2940 (2015).

44. Tully, D. C., Liu, H., Chatterjee, A. K., Alper, P. B., Williams, J. A., Roberts, M. J., Mutnick, D., Woodmansee, D. H., Hollenbeck, T., Gordon, P., Chang, J., Tuntland, T., Tumanut, C., Li, J., Harris, J. L. & Karanewsky, D. S. Arylaminoethyl carbamates as a novel series of potent and selective cathepsin S inhibitors. *Bioorg. Med. Chem. Lett.* **16,** 5107–5111 (2006).